

Order-Reduction Abstractions for Safety Verification of High-Dimensional Linear Systems

Hoang-Dung Tran, Luan Viet Nguyen,
Weiming Xiang, Taylor T. Johnson

Received: February 15, 2016 / Accepted: date

Abstract Order-reduction is a standard automated approximation technique for computer-aided design, analysis, and simulation of many classes of systems, from circuits to buildings. For a given system, these methods produce a reduced-order system where the dimension of the state-space is smaller, while attempting to preserve behaviors similar to those of the full-order original system. To be used as a sound abstraction for formal verification, a measure of the similarity of behavior must be formalized and computed, which we develop in a computational way for a class of linear systems and periodically-switched systems as the main contributions of this paper. We have implemented the order-reduction as a sound abstraction process through a source-to-source model transformation in the HyST tool and use SpaceEx to compute sets of reachable states to verify properties of the full-order system through analysis of the reduced-order system. Our experimental results suggest systems with on the order of a thousand state variables can be reduced to systems with tens of state variables such that the order-reduction overapproximation error is small enough to prove or disprove safety properties of interest using current reachability analysis tools. Our results illustrate this approach is effective to alleviate the state-space explosion problem for verification of high-dimensional linear systems.

Keywords Abstraction; model reduction; order reduction; verification; reachability analysis

1 Introduction

The state-space explosion problem is a fundamental challenge in model checking and automated formal verification that has received significant attention from the verification community. Roughly, the state-space explosion problem is that the size of the state-space of systems scales exponentially or combinatorially with their dimensionality, which in turns causes formal computational analyses of these systems to scale similarly. Among many solutions, abstractions based on the concepts of exact and approximate simulation and bisimulation relations are effective approaches to

University of Texas at Arlington, USA

obtain smaller state spaces by abstracting away information that is not needed in the verification process. Such abstractions have been applied broadly to simplify the controller synthesis and safety verification process of complex systems. Applications of these abstractions can be found in many fields such as embedded systems [Hen-zinger and Sifakis (2006)], biological systems [Danos and Laneve (2004); Regev et al. (2004); Asarin and Dang (2004)], continuous and hybrid systems models of cyber-physical systems (CPS) [Alur et al. (2000); Belta et al. (2005); Girard and Pappas (2007b); Girard et al. (2008)], and stochastic systems [Wang et al. (2015)].

Model reduction techniques have been developed and applied widely in controls [Antoulas et al. (2001)], but are typically approximations and not sound abstractions that may be used in formal verification. From a high-dimensional (“full-order”) original system, model reduction can obtain automatically a simplified (“reduced-order”) system with lower-dimensionality that is computationally easier to, for example, analyze, design controllers for, and simulate.

A key difference between model reduction and abstraction relies on dealing with the system’s initial condition and inputs. In model reduction, the inputs’ values remain the same and the initial set of system states, which is an important factor in verification with reachability analysis, is usually assumed to be the zero set. Thus, order reduction may not be sound as it is an approximation that may not have bounded errors and may be subject to numerical errors, while a guaranteed error bound (“conservative approximation”) is necessary to define a sound abstraction for verification. In contrast, the initial condition is always taken into account and the inputs’ values may change in the context of bisimulation-based abstraction.

In order to be able to use model reduction as a sound abstraction for formal verification, we need to consider both the initial conditions and inputs and then present additional reasoning to derive error bounds for how far off the executions of the reduced-order system may be from those of the full-order system. Formalizing these issues and addressing them is the main objective of this paper, which we then use to derive an automated order-reduction abstraction that is sound, and use it to verify high-dimensional (with upwards of hundreds to thousands of state variables) continuous and periodically switched systems.

1.1 Related Work

Exact bisimulation relation-based abstractions for safety verification and controller synthesis have been investigated widely in the last decade [Pappas (2003); van der Schaft (2004); Tanner and Pappas (2003); Tabuada and Pappas (2004)]. In this context, the outputs of the the abstract system capture exactly the outputs of the original system. As pointed out in [Girard et al. (2008); Girard and Pappas (2007a)], the term of “exact” is not adequate when dealing with continuous and hybrid systems observed over real numbers since there may be numerical errors in observation, noise, among other nonidealities. To obtain an abstraction that guarantees more robust relationships between systems, approximate bisimulation relations have been proposed and studied extensively in recent years [Girard and Pappas (2005); Girard et al. (2008); Girard and Pappas (2007a); Julius (2006); Girard et al. (2006); Islam et al. (2015)]. The main advantage of such approximate relations is that they allow a bounded error δ which describes how far off the executions of the abstraction may be from those of the original system. Then, verifying whether the executions of the

original system reach an unsafe region U can be turned out to verify whether the executions of the abstraction (with much lower dimension) reach the δ -neighborhood of the unsafe region U . Thus, finding an efficient way to determine a tight bound of the error becomes an essential task for this approach. In particular, a computation framework has been proposed and integrated in a Matlab toolbox called Matisse to find an abstraction from the original linear system and calculate the bound of their output mismatch [Girard and Pappas (2007a)]. Note that in [Girard and Pappas (2007a)], the error bound is called as a precision. The proposed method shows a great benefit when it can deal both stable and unstable systems. In this framework, computing the error bound is basically based on solving a set of linear matrix inequality (LMI) and optimization problem on the sets of initial states and inputs. The computation complexity increases polynomially along with the size of the system. In addition, in some cases, due to the ill-condition of some matrices in computation process, the error bound computed may be very conservative and thus may produce an abstraction that is not useful for verification.

Model reduction techniques have been applied for formal verification of continuous and hybrid system [Han and Krogh (2004); Han (2005)]. These techniques rely on output reach sets, which combines the set of reachable states and an observation matrix. This concept is useful in safety verification because, for a given system, we are usually interested in the safety requirements of some specific important states or their combinations which can be declared as the outputs of the system. Particularly, the authors use a reduced-order model and its output error bound compared with full-order model to overapproximate the output reach set of the original system [Han and Krogh (2004)]. Thus, determining a tight bound of the error is essential. Intuitively, the error between full-order model and its reduced-order model is composed of two separate errors. The first error corresponds to the zero-input response (i.e., there is no control input) and the second error corresponds to the zero-state response (i.e., the initial state of the system is zero). The authors use simulation to determine the bounds of these errors before combining them as a total bound. The first error bound is determined by simulating the the full-order system and the reduced model from each vertex of a polyhedral initial set of states. The advantages of simulation is it can derive tight bounds of these errors. The drawback of using simulation is the number of simulations increases exponentially with the dimension of the polyhedron, since the number of vertices of a polyhedron increases exponential with the dimensionality (for example, an n -dimensional hyperbox has 2^n vertices). Thus, it may be infeasible to perform enough simulations for a high-dimensional system.

Reachability analysis of large-scale affine systems has also been investigated with Krylov subspace approximation methods to deal with state-space explosion [Han and Krogh (2006)]. However, this approach requires the input to the system to be constant, while in contrast, in our work, we consider a more general class of systems with varying inputs.

Contributions and Organization. In this paper, we develop the order-reduction abstraction for safety verification of high-dimensional linear systems. The main contributions of this paper are: (a) a computationally efficient method to derive an output abstraction from high-dimensional linear systems with an error bound for each element of the outputs, where this error is essentially the sum of two separate errors caused by the initial set of states and the control inputs; (b) establishing soundness of using this output abstraction to verify the safety requirements of the original sys-

tem with a significantly lower computation cost; (c) an extension of these results to a class of periodically switched linear systems; and (d) the implementation of the methods as a model transformation pass within the HyST model transformation tool [Bak et al. (2015)], along with a thorough evaluation comparing our approach to similar existing order-reduction and approximate bisimulation-based abstraction methods.

Our computational framework has been tested and compared in detail with similar results through a set of benchmarks [Girard and Pappas (2007a); Han and Krogh (2004)]. Our empirical evaluation illustrates that our method not only works efficiently for small and medium-dimensional systems (several to less than a hundred dimensions) as existing methods [Girard and Pappas (2007a); Han and Krogh (2004)], but also can be applied to high-dimensional systems (with a hundred to a thousand dimensions) where the existing methods are infeasible to apply due to either computational complexity or finding overly conservative error bounds. The error bound value and computation time of these different methods have been compared and discussed in our paper to show the advantages and tradeoffs of our approach.

Besides improving the computational framework, we also establish soundness of our method using the output abstraction to verify the safety specifications of the original full-order system using an approximate bisimulation relation argument. In [Girard and Pappas (2007a)], the authors use the general concept of set neighborhood to transform the safety specification of the original system. However, in some cases when the safe and unsafe regions are described by polytopes or ellipsoids that are often used, for example in SpaceEx [Frehse et al. (2011)] and the Ellipsoid Toolbox [Kurzghanskiy and Varaiya (2006)], a more precise transformed safety specification can be derived by our element-to-element approach. The transformed safety specification need to satisfy the following safety relation property: (1) if the output abstraction is safe (i.e., it satisfies the transformed safety specification), then the original system is safe, and (2) if the abstraction is unsafe (it does not satisfy the transformed safety specification), then the original system is unsafe. Since we verify safety using the output abstraction, the computation cost of the verification process is significantly reduced. Moreover, our approach is very useful for verifying safety of high-dimensional systems that the existing verification tools may not successfully analyze directly. This improvement is shown through our evaluation of computation complexity of safety verification for the original full-order system and its different output abstractions (Section 6, Table 5). Our method has been implemented as a source-to-source model transformation in the HyST tool [Bak et al. (2015)], which makes it easy to combine different verification tools, such as SpaceEx [Frehse et al. (2011)], Flow* [Chen et al. (2013)] and dReach [Kong et al. (2015)] to verify safety property of high-dimensional linear systems.

The remainder of the paper is organized as follows. Section 2 gives definitions of output reach set, output abstraction, safety specification, safety verification problem and safety specification transformation for a class of linear time invariant (LTI) systems. Section 3 presents methods to find output abstractions of the LTI systems using the balanced truncation model reduction method. Section 4 discusses how to verify safety properties for a full-order LTI system using its output abstraction. Section 5 extends the results to a class of periodically switched systems in which the state of the system is re-initialized at every switching instance. Section 6 describes our implementation of the method in a prototype tool, and presents a number of examples to illustrate and evaluate the benefits of our method.

2 Preliminaries

In this section, we introduce definitions used throughout the paper including output reach sets [Han and Krogh (2004)], output abstractions, safety specifications, the safety verification problem, and safety specification transformation.

Definition 1 An n -dimensional LTI system is denoted $M_n(y|\{x, u\})\langle A, B, C \rangle$ (written in short as M_n). It has the following dynamic equations:

$$\begin{aligned}\dot{x}(t) &= Ax(t) + Bu(t) \\ y(t) &= Cx(t),\end{aligned}$$

where $x(t) \in \mathbb{R}^n$ is the *system state*, $y(t) \in \mathbb{R}^p$ is the *system output*, $u(t)$ is the *control input*, $A \in \mathbb{R}^{n \times n}$, $B \in \mathbb{R}^{n \times m}$, and $C \in \mathbb{R}^{p \times n}$.

The initial set of states of M_n is denoted by $X_0(M_n) \subseteq \mathbb{R}^n$, and we write initial conditions as $x(0) \in X_0(M_n)$. The set of control inputs of M_n is $U \subseteq \mathbb{R}^m$, and we write particular controls as $u(t) \in U$. The state of M_n is updated from state x to the new state x' over intervals of real time according to the linear differential equation $Ax + Bu$, and the *behaviors* of the system is defined in this paper as the trajectories of the output $y(t)$ over intervals of real time.

Next, we present the output reach set defined in related approaches using order reduction as a sound abstraction [Han and Krogh (2004)].

Definition 2 Output Reach Set [Han and Krogh (2004)]. Given an LTI M_n , a set of control inputs U , and an initial set $X_0(M_n)$, the *output reach set at a time instant t* is:

$$R_t(M_n) \triangleq \{y(t, u, x_0) | y(t, u, x_0) = Ce^{At}x_0 + \int_{t_0}^t Ce^{A(t-\tau)}Bu(\tau)d\tau\},$$

where $x_0 \in X_0(M_n)$ and $u(t) \in U$.

The *output reach set over an interval of time $[t_0, t_f]$* for $t_0 \leq t_f$ is:

$$R_{[t_0, t_f]}(M_n) \triangleq \bigcup_{t \in [t_0, t_f]} R_t(M_n).$$

In the remainder of the paper, we suppose $t_0 = 0$. Next, we define an output abstraction, which is a formalization of the reduced-order system that will be used to verify properties of the full-order system.

Definition 3 Output Abstraction. The k -dimensional LTI system M_k^δ , $p < k \leq n$ described by:

$$\begin{aligned}\dot{x}_r(t) &= A_r x_r(t) + B_r u(t), \\ y_r(t) &= C_r x_r(t),\end{aligned}$$

where $x_r(t) \in \mathbb{R}^k$, $y_r(t) \in \mathbb{R}^p$, $A_r \in \mathbb{R}^{k \times k}$, $B_r \in \mathbb{R}^{k \times m}$, $C_r \in \mathbb{R}^{p \times k}$, is called a *k -dimensional output abstraction of M_n* if, for the *error bound* $\delta = [\delta_1, \delta_2, \dots, \delta_p]^T$, where each δ_i is a finite positive real, we have:

1. $\forall x(0) \in X_0(M_n)$ and $u \in U$, $\exists x_r(0) \in X_0(M_k^\delta)$ such that, $\forall t \geq 0$, $\|y^i(t) - y_r^i(t)\| \leq \delta_i$, $1 \leq i \leq p$.

where $y^i(t)$ is the i^{th} component of the output y at time t , and $\|\cdot\|$ denotes the Euclidean norm.

If we can find an output abstraction M_k^δ , then its behaviors will approximate within δ the behaviors of the full-order system M_n for all time.

Definition 4 Safety Specification. A *safety specification* $S(M_n)$ of an LTI system M_n formalizes the safety requirements for the output y of M_n , and is a predicate over the output y of M_n . Formally, $S(M_n) \subseteq \mathbb{R}^p$.

Definition 5 Safety Verification. The *time-bounded safety verification problem* is to verify whether the system M_n satisfies a safety specification $S(M_n)$ over an *interval of time*. Whether M_n is safe or unsafe is defined over an *interval of time* $[0, t_f]$, which is described formally in terms of the output reach set as:

$$\begin{aligned} R_{[0, t_f]}(M_n) \cap \neg S(M_n) = \emptyset &\Leftrightarrow M_n \models S(M_n), \\ R_{[0, t_f]}(M_n) \cap \neg S(M_n) \neq \emptyset &\Leftrightarrow M_n \not\models S(M_n). \end{aligned}$$

In the remainder of the paper, we will assume t_f is finite and focus on time-bounded safety verification, albeit the general framework we develop and error bounds we derive are applicable to time-unbounded verification where $t_f \rightarrow \infty$. Under this assumption, we fix t_f to some positive real. If M_n satisfies $S(M_n)$, then it is *safe* and we write $M_n \models S(M_n)$. If M_n does not satisfy $S(M_n)$, then it is *unsafe* and we write $M_n \not\models S(M_n)$.

Definition 6 Safety Specification Transformation. The *safety specification transformation* is the process of finding the corresponding safety (or dually, unsafe) specification for the output abstraction M_k^δ denoted by $S(M_k^\delta) \in \mathbb{R}^p$ (and dually $U(M_k^\delta) \in \mathbb{R}^p$) from the safety specification $S(M_n)$ of the full-order system M_n to guarantee the safety relation defined by:

$$\begin{aligned} R_{[0, t_f]}(M_k^\delta) \cap \neg S(M_k^\delta) = \emptyset &\Rightarrow M_n \models S(M_n), \\ R_{[0, t_f]}(M_k^\delta) \cap U(M_k^\delta) \neq \emptyset &\Rightarrow M_n \not\models S(M_n). \end{aligned} \tag{1}$$

3 Output Abstractions from Balanced Truncation Reduction

The balanced truncation model reduction is an effective method to find reduced models for large scale systems. Balanced truncation is based on Singular Value Decomposition (SVD) [Moore (1981)] and uses a balanced projection to transform a system to an equivalent *balanced system* where the states are arranged in descending degrees of their controllability and observability. Informally, the degrees of controllability and observability are measures to check how controllable and observable a given system is. For further details, we refer readers to [Moore (1981); Silverman and Meadows (1967)]. The k -order reduced model is then obtained by selecting the first k states in the state vector and truncating (i.e., projecting away or eliminating) the other $n - k$ states. The process of determining the reduced-order model's matrices is well-known, and it is briefly described here. We refer readers to [Moore (1981)] for further details.

3.1 Order Reduction with Balanced Truncation Method

For an LTI system M_n , the controllability gramian W_c and observability gramian W_o of M_n are the solutions of the following Lyapunov equations,

$$\begin{aligned} AW_c + W_c A^T + BB^T &= 0 \\ A^T W_o + W_o A + C^T C &= 0. \end{aligned}$$

It should be noticed that W_c and W_o are symmetric and positive definite. The Hankel singular value σ_i is defined as the square root of each eigenvalue λ_i of $W_c W_o$,

$$\sigma_i = (\lambda_i(W_c W_o))^{\frac{1}{2}}.$$

The first step in balanced model reduction method is to implement a balanced transformation $\tilde{x}(t) = Hx(t)$, $H \in \mathbb{R}^n$ to transform M_n to an equivalent balanced system \tilde{M}_n , where the controllability and observability gramian \tilde{W}_c, \tilde{W}_o satisfy:

$$\tilde{W}_c = \tilde{W}_o = \Sigma = \begin{pmatrix} \sigma_1 & & & \\ & \sigma_2 & & \\ & & \ddots & \\ & & & \sigma_n \end{pmatrix},$$

for $\sigma_1 \geq \sigma_2 \geq \sigma_3 \geq \dots \geq \sigma_{n-1} \geq \sigma_n$. The transformation matrix H can be computed as follows.

Since W_c is symmetric and positive definite, we can factor it as $W_c = GG^T$, where G is invertible. There exists an orthogonal transformation K , (i.e. $KK^T = I$, where I is an identity matrix) such that $G^T W_o G = K \Sigma^2 K^T$. Then, the transformation matrix H is defined as:

$$H = \Sigma^{\frac{1}{2}} K^T G^{-1}.$$

Applying transformation to the system M_n , we have the equivalent balanced system \tilde{M}_n with:

$$\begin{aligned} \dot{\tilde{x}}(t) &= \tilde{A}\tilde{x}(t) + \tilde{B}u(t) \\ y(t) &= \tilde{C}\tilde{x}(t), \end{aligned}$$

where $\tilde{A} = HAH^{-1}$, $\tilde{B} = HB$ and $\tilde{C} = CH^{-1}$. The matrices of \tilde{M}_n can be partitioned as:

$$\tilde{A} = \begin{pmatrix} \tilde{A}_{11} & \tilde{A}_{12} \\ \tilde{A}_{21} & \tilde{A}_{22} \end{pmatrix}, \tilde{B} = \begin{pmatrix} \tilde{B}_1 \\ \tilde{B}_2 \end{pmatrix}, \tilde{C} = (\tilde{C}_1 \quad \tilde{C}_2),$$

where $\tilde{A}_{11} \in \mathbb{R}^{k \times k}$, $\tilde{B}_1 \in \mathbb{R}^{k \times m}$, and $\tilde{C}_1 \in \mathbb{R}^{p \times k}$, and the other matrices are of appropriate dimensionality. Finally, the k -dimensional reduced system M_k of M_n is defined as:

$$\begin{aligned} \dot{x}_r(t) &= A_r x_r(t) + B_r u(t) \\ y_r(t) &= C_r x_r(t). \end{aligned} \tag{2}$$

where $A_r = \tilde{A}_{11}$, $B_r = \tilde{B}_1$ and $C_r = \tilde{C}_1$. The initial set of M_k is $X_0(M_k) = \{SHx_0 | x_0 \in X_0(M_n)\}$, where $S = \begin{pmatrix} I_{k \times k} & 0_{k \times (n-k)} \end{pmatrix}$.

The balanced truncation method obtains the system matrices of the k -dimensional reduced system. Next, we investigate the error between the outputs of the full-order system and its k -dimensional reduced system.

3.2 Determining the Error Bound δ

The solution of a LTI system can be decomposed into two parts. The first part corresponds to zero control input (i.e. $u(t) = 0$ for all t) and the second part corresponds to zero initial state (i.e., $x_0 = 0$). Note that $x_0 \equiv x(t = 0)$. The solutions of M_n and M_k are given as follows:

$$\begin{aligned} y(t) &= y_0 + y_u(t), \quad y_r(t) = y_{r_0}(t) + y_{r_u}(t) \\ y_0(t) &= Ce^{At}x_0, \quad y_u(t) = \int_0^t Ce^{A(t-\tau)}Bu(\tau)d\tau \\ y_{r_0}(t) &= C_re^{A_rt}x_{r_0}, \quad y_{r_u}(t) = \int_0^t C_re^{A_r(t-\tau)}B_ru(\tau)d\tau \\ x_0(t) &\in X_0(M_n), \quad x_{r_0}(t) \in X_0(M_k), \quad u(\tau) \in U. \end{aligned}$$

The error between the full-order system M_n and its k -dimensional reduced system M_k at time t is given as follows:

$$\begin{aligned} e(t) &= y(t) - y_r(t) = e_1(t) + e_2(t), \text{ where} \\ e_1(t) &= y_0(t) - y_{r_0}(t), \text{ and } e_2(t) = y_u(t) - y_{r_u}(t). \end{aligned} \quad (3)$$

The error e_1 relates to the zero input state responses of the full-order system and the output abstraction; that is, the responses are only caused by the initial set of states. The error e_2 relates to the zero state responses; that is, the responses are only caused by the control inputs. Note that e_1 and e_2 are both time varying and $e_1(t), e_2(t) \in \mathbb{R}^p$ where p is the output dimensionality.

To obtain our main results in computing the error bounds, in the rest of this paper, we consider the $(n + k)$ -dimensional augmented system as follows,

$$\begin{aligned} \dot{\bar{x}} &= \bar{A}\bar{x} + \bar{B}u = \begin{pmatrix} \bar{A} & 0 \\ 0 & A_r \end{pmatrix} \bar{x} + \begin{pmatrix} \bar{B} \\ B_r \end{pmatrix} u, \\ \bar{y} &= \bar{C}\bar{x} = (\bar{C} \quad -C_r) \bar{x}, \end{aligned}$$

where $\bar{x} = (Hx \quad SHx)^T$.

It is easy to see that the output of the augmented system is the error between the n -dimension full-order system and its k -dimensional reduced system. Thus, determining the error bound δ is equivalent to determining the bounds of the augmented system's outputs in which the bound of e_1 corresponds to the zero input response, while the bound of e_2 relates to the zero state response of the augmented system.

A theoretical bound of e_1 can be given with the following theorem.

Theorem 1 *Let $\bar{x}_0 = (Hx_0 \quad SHx_0)^T$, then the error e_1 between the full-order system M_n and its k -dimensional reduced system M_k satisfies the following inequality for all $t \in \mathbb{R}_{\geq 0}$:*

$$\|e_1^i(t)\| \leq \lambda_{max}(\bar{C}_i^T \bar{C}_i) \cdot \sup_{x_0 \in X_0} \|\bar{x}_0\|, \quad 1 \leq i \leq p,$$

where $\mathbb{R}_{\geq 0}$ is the set of non-negative real numbers, \bar{C}_i is the row i of the matrix \bar{C} , and $e_1^i(t)$ is the i^{th} element of vector $e_1(t)$.

The proof of Theorem 1 is given in Appendix 8.1.

Although the computation cost of the theoretical bound of e_1 is small since it only relates to determining $\sup_{x_0 \in X_0} \|\bar{x}_0\|$, the result may be very conservative in the case that the initial set of states is far from the zero point. Thus, as can be seen in Section 6, it is efficient to use Theorem 1 to compute the bound of e_1 if the initial set of states is close to zero point.

To reduce the conservativeness of Theorem 1, we also propose an optimization method to compute a tighter bound of e_1 . Nevertheless, the computation cost of the optimization method is larger than using Theorem 1. This is the tradeoff between obtaining an accuracy bound of e_1 and improving the computation time. An optimization method is given in the following theorem.

Theorem 2 *Let $\bar{x}_0 = (Hx_0 SHx_0)^T$ and $P_0 > 0$ is the solution of the following optimization problem:*

$$\begin{aligned} P_0 &= \min(\text{trace}(P)) \text{ subject to} \\ P &> 0, \bar{A}^T P + P A < 0, \bar{C}_i^T \bar{C}_i \leq P \end{aligned}$$

where \bar{C}_i is the row i of the matrix \bar{C} . Then, the error e_1 between the full-order system M_n and its k -dimensional reduced system M_k satisfies the following inequality for all $t \in \mathbb{R}_{\geq 0}$:

$$\|e_1^i(t)\| \leq \sup_{x_0 \in X_0} \sqrt{\bar{x}_0^T P_0 \bar{x}_0}, \quad 1 \leq i \leq p,$$

where $e_1^i(t)$ is the i^{th} element of vector $e_1(t)$.

The proof of Theorem 2 is given in Appendix 8.1.

Now, we consider how to determine the bound of e_2 , which corresponds to the zero state responses of the augmented system. The theoretical bound of e_2 is obtained in the following theorem by exploiting the concept of bounded input bounded output stability (BIBO) and the L_1 error bound in the impulse response of balanced truncation model reduction [Obinata and Anderson (2012)].

Theorem 3 *The error e_2 between the full-order system M_n and its k -dimensional reduced system M_k satisfies the following inequality for all $t \in \mathbb{R}_{\geq 0}$:*

$$\|e_2^i(t)\| \leq (2 \sum_{j=k+1}^n (2j-1)\sigma_j) \cdot \|u\|_{\infty}, \quad 1 \leq i \leq p,$$

where $e_2^i(t)$ is the i^{th} element of vector $e_2(t)$.

The proof of Theorem 3 is given in Appendix 8.1.

Remark 1 As can be observed from Theorem 3, the theoretical bound of e_2 depends on the singular value σ_j , $k+1 \leq j \leq n$. Therefore, in the case of the singular values are large, the theoretical bound of e_2 becomes large and may be not useful. Moreover, Theorem 3 derives the same error bounds e_2^i for each pair $(y_u^i, y_{r_u}^i)$ for each dimension $1 \leq i \leq p$. Thus, Theorem 3 may be more useful for systems that have high dimensions and small singular values.

After determining the bounds e_1 and e_2 , the overall error bound $\delta = [\delta_1, \delta_2, \dots, \delta_p]^T$ between the outputs of M_n and M_k obtained from (3) can be expressed as follows:

$$\|y_i(t) - y_{r,i}(t)\| \leq \delta_i, \quad 1 \leq i \leq p. \quad (4)$$

where $\delta_i = \|e_1^i(t)\| + \|e_2^i(t)\|$.

Remark 2 We note that the bound δ can be obtained using different methods in which each method has both benefits and drawbacks. For example, in contrast to our above results, in [Han and Krogh (2004)], the authors propose a simulation-based approach to determine these error bounds. To determine the bound of e_1 , the author simulate the full-order system and the reduced system from each vertex in a polyhedral representation of the initial set of states. This method gives a very tight bound of e_1 . The drawback is the number of simulations may explode. For example, if the initial set is a hypercube in 100-dimensions, we have to simulate the full-order system and its reduced system with $2^n = 2^{100}$ vertices, which is infeasible even if each simulation takes little time. The bound of e_2 is determined by integrating the norm of the impulse response of the augmented system via simulation. This method is useful since it gives a tight bound of e_2 with only m simulations, where m is the number of inputs. In a different way without separately computing the bounds of e_1 and e_2 , the error bound δ can be calculated by solving a set of LMI optimization problem on sets of initial states and inputs [Girard and Pappas (2007a)]. This approach shows advantages when dealing with small and medium-dimensional systems (less than 50 dimensions) and it works for both stable and unstable systems. When the system dimension is large, the error bound obtained is overly conservative and may not be useful.

Discussion. Although simulation-based methods can be used to determine the bounds of e_1 and e_2 , numerical issues in simulation may lead to unexpected results (unsound results) which are smaller than the actual error bounds. Let us clarify the problem first and then propose a technique under an assumption to make the result obtained via simulation sound. This problem has not been addressed previously in [Han and Krogh (2004)].

Assume that the actual values of the bounds of e_1 and e_2 are \bar{e}_1 and \bar{e}_2 respectively, and the values of error bounds we get from simulation are \tilde{e}_1 and \tilde{e}_2 . The numerical inaccuracy in simulation can be formulated as $\bar{e}_1 = \tilde{e}_1 \pm \epsilon_1$ and $\bar{e}_2 = \tilde{e}_2 \pm \epsilon_2$. The actual overall bound δ is $\bar{e}_1 + \bar{e}_2$ which satisfies the following constraint:

$$\delta = \bar{e}_1 + \bar{e}_2 = \tilde{e}_1 + \tilde{e}_2 \pm \epsilon_1 \pm \epsilon_2.$$

From the above equation, it is easy to see that if we use the simulation bounds of e_1 and e_2 to calculate δ , then the result may be unsound due to numerical issues (i.e. if $\pm\epsilon_1 \pm \epsilon_2 > 0$). To handle this, we can assume that the absolute numerical error in simulation $|\epsilon_i|$, $i = 1, 2$ is smaller than γ percent of the simulation value \tilde{e}_i , $i = 1, 2$. Then, the simulation error bound can be used as a sound result by bloating the simulation error bound using following equation.:

$$\delta = (1 + \gamma)(\tilde{e}_1 + \tilde{e}_2).$$

The soundness of error bounds δ computed using Theorem 1, Theorem 2, Theorem 3, and the methods of [Girard and Pappas (2007a)] are guaranteed since these methods do not have numerical issues that may arise in simulation-based methods.

3.3 Output abstraction and δ -approximation relation

Lemma 1 *Given an asymptotically stable LTI system M_n , there exists a k -dimensional output abstraction M_k^δ of M_n .*

Proof Assume that we have an asymptotically stable LTI system M_n , using balanced truncation method in Section 3.1, we can obtain a k -dimensional reduced system M_k . Moreover, from Section 3.2, for any $x(0) \in X_0(M_n)$, there exists $x_r(0) = SHx(0) \in X_0(M_k)$ such that the distance between each pair of output $(y_i(t), y_{r,i}(t))$ of the two systems is bounded by a finite positive real δ_i , and this applies in every dimension $1 \leq i \leq p$ (4). Hence, we can conclude that there exists a k -dimensional output abstraction $M_k^\delta(y_r|\{x_r, u\}) \langle A_r, B_r, C_r \rangle$ of M_n .

There is a relationship between the output abstraction and δ -approximate (bi)simulation relations [Girard and Pappas (2007a)] given as follows.

Consider two dynamic systems:

$$\begin{aligned} \Sigma : \dot{x}(t) &= f_1(x(t), u(t)), \\ y(t) &= g_1(x(t)), \\ \tilde{\Sigma} : \dot{\tilde{x}}(t) &= f_2(\tilde{x}(t), u(t)), \\ \tilde{y}(t) &= g_2(\tilde{x}(t)). \end{aligned}$$

The central notion of approximate bisimulation is to characterize and quantify the distance between the outputs $y(t)$ and $\tilde{y}(t)$ generated by system Σ and $\tilde{\Sigma}$ with the same input $u(t)$.

Definition 7 [Girard and Pappas (2007a)] A relation $\mathcal{R}_\delta \subseteq \mathbb{R}^{n_x} \times \mathbb{R}^{\tilde{n}_x}$ is called a δ -approximate bisimulation relation between systems Σ and $\tilde{\Sigma}$, of *precision* δ , if, $\forall t \in \mathbb{R}_{\geq 0}$ and for all $(x(t), \tilde{x}(t)) \in \mathcal{R}_\delta$:

1. $\|y(t) - \tilde{y}(t)\| \leq \delta$,
2. $\forall u(t) \in \mathcal{U}$, \forall solutions $x(t)$ of Σ , \exists a corresponding solution $\tilde{x}(t)$ of $\tilde{\Sigma}$ such that $(x(t), \tilde{x}(t)) \in \mathcal{R}_\delta$,
3. $\forall u(t) \in \mathcal{U}$, \forall solutions $\tilde{x}(t)$ of $\tilde{\Sigma}$, \exists a corresponding $x(t)$ of Σ such that $(x(t), \tilde{x}(t)) \in \mathcal{R}_\delta$.

If these conditions are met, we say systems Σ and $\tilde{\Sigma}$ are approximately bisimilar with precision δ , denoted by $\Sigma \sim_\delta \tilde{\Sigma}$.

Parameter δ measures the similarity of two systems Σ and $\tilde{\Sigma}$. In particular, \mathcal{R}_0 with $\delta = 0$ recovers the exact bisimulation relation. However, in most situations, the value of δ has to be greater than zero for two bisimilar systems, then the problem of calculating a tight estimate of δ is of the most importance in using approximate bisimulation relations for verification.

In this context, we relate the precision δ with the overall error bound $\delta = [\delta_1, \delta_2, \dots, \delta_p]^T$ developed earlier (4), to obtain the following proposition to establish an approximate bisimulation relation between the full-order system M_n and its output abstraction M_k^δ .

Proposition 1 *For the full-order LTI system $M_n(y|\{x, u\}) \langle A, B, C \rangle$ and the k -reduced order system $M_k(y_r|\{x_r, u\}) \langle A_r, B_r, C_r \rangle$ by (2), there exists an approximate bisimulation relation \mathcal{R}_ρ such that $M_n \sim_\rho M_k$, where $\rho = \|\delta\|$.*

Proof For output $y(t)$ and $y_r(t)$ generated by M_n and M_k , we have:

$$\|y(t) - y_r(t)\| = \sqrt{\sum_1^p (y^i(t) - y_r^i(t))^2}.$$

Then, with the error bound δ_i , $i = 1, 2, \dots, p$, computed by (4), we have:

$$\|y(t) - y_r(t)\| \leq \sqrt{\sum_1^p \delta_i^2} = \|\delta\| = \rho.$$

According to Definition 7, and by either Theorem 1 or Theorem 2 for the e_1 error bound and by Theorem 3 for the e_2 error bound, the approximate bisimulation relation \mathcal{R}_ρ with precision ρ is established.

Remark 3 It should be emphasized that there is a difference between the output abstraction and the δ -approximate bisimulation relation since we compute the distance element to element between the outputs of two systems, i.e., $\|y_i - y_{r,i}\| \leq \delta_i$. Our more precise result can produce a tighter transformed safe and unsafe specifications, which will be clarified in the next section.

3.4 Computational time complexity to compute the error bound

Assume that the average time for one simulation is \bar{t} , then the time for the simulation-based approach [Han and Krogh (2004)] to compute the error bound will be $\bar{t} \times N$, where N is the total number of simulations. To analyze the time complexity of the simulation-based approach, we need to determine N . For an n -dimension system with m inputs and p outputs, the number of vertices in polyhedral initial set is 2^n . Therefore, the number of simulations that need to be done to determine the bound of e_1 is 2^n . Similarly for e_2 , as discussed in the previous section, the number of simulations for determining the bound of e_2 is m . Overall, the number of simulations N need to be done in the worst case is $N = 2^n + m$, and the overall simulation time needed is $O(\bar{t} \times (2^n + m))$.

In [Girard and Pappas (2007a)], to compute the error bound, this method solves two LMI and quadratic optimization problems on the sets of initial state and inputs. To estimate the time complexity of this method, we need to calculate the number of decision variables first. For the n -dimensions system, the number of decision variables is $(n^2 + n)/2$. The number of LMI constraints related to this method is 2. Consequently, the time complexity for solving two LMI constraints using interior point algorithms can be estimated by $O([(n^2 + n)/2]^{2.75} \times 2^{1.5})$ [Vandenberghe and Boyd (1994); Nesterov et al. (1994)]. The time complexity for solving the optimization problem in [Girard and Pappas (2007a)] using interior point algorithms is $O([(n^2 + n)/2]^3)$ [Vandenberghe and Boyd (1994); Nesterov et al. (1994)]. Totally, the time complexity in computing the error bound of the method proposed in [Girard and Pappas (2007a)] is $O([(n^2 + n)/2]^3) + O([(n^2 + n)/2]^{2.75} \times 2^{1.5})$, which can be bounded as $O(n^6)$.

In our approach, it is easy to see that Theorem 1 computation mainly relates to solving the optimization problem to find $\sup_{x_0 \in X_0} \|\bar{x}_0\|$. This optimization problem can be done in two steps. The first step is to find the upper bound and lower bound of \tilde{x}_0 by solving the linear optimization problem defined by $\min(\max) Hx_0$, $x_0 \in X_0$.

[Girard and Pappas (2007a)]	$O(n^6)$
[Han and Krogh (2004)]	$O(2^n + m)$
Theorem 1	$O(n^{3.5})$
Theorem 2	$O((n+k)^{5.5})$

Table 1: Time complexity of different methods to compute the error bound δ .

Then, the supremum of the Euclidean-norm of \bar{x}_0 can be easily obtained. If we use interior point algorithms for this problem, the time complexity of our approach using Theorem 1 is $O((n+1)^{3.5})$ [Nesterov et al. (1994)]. If we use the optimization method proposed in Theorem 2, we first need to solve the eigenvalue problem (EVP) subject to two matrix inequalities that has time complexity $O(((n+k)^2 + n + k)/2)^{2.75} \times 2^{1.5})$ if using interior point algorithms [Vandenberghe and Boyd (1994)]. Then, we need to solve the quadratic optimization problem that has time complexity $O((n+k)^3)$ if we use the interior point algorithm [Ye and Tse (1989)]. Note that the computation cost of Theorem 3 in our approach is small compared to Theorem 1 and Theorem 2.

Table 1 shows the simplified time complexity analysis of different approaches to compute the error bound δ . As can be seen from the above discussion and Table 1, in terms of time complexity, our approach using Theorem 1 and Theorem 3 is more efficient when dealing with high-dimensional systems while using Theorem 2 does not improve the time complexity. The computation time of different methods are measured and discussed in detail in Section 6.

4 Safety Verification with Output Abstractions

In this section, we focus on answering two critical questions: (a) how can an output abstraction be used to verify safety specifications of the original, full-order system? (b) How can an appropriate output abstraction be derived automatically? To answer the first question, safety specifications must be transformed from those over the states of the full-order system to its output abstraction.

For the general approximate bisimulation relation $\Sigma \sim_\delta \tilde{\Sigma}$, we usually use δ -neighborhood to transform the safe and unsafe set.

Proposition 2 *If $\Sigma \sim_\delta \tilde{\Sigma}$, then the following statements are true:*

1. System Σ is safe if $R_{[t_0, t_f]}(\tilde{\Sigma}) \cap \mathcal{N}(U(\Sigma), \delta) = \emptyset$
2. System Σ is unsafe if $R_{[t_0, t_f]}(\tilde{\Sigma}) \cap \mathcal{N}(S(\Sigma), \delta) \neq \emptyset$

where $\mathcal{N}(\cdot, \delta)$ denotes the δ -neighborhood of a set.

Remark 4 δ -neighborhood is a general approach to transform safety specification. However, in some cases when the safe and unsafe specifications are describes by polytopes or ellipsoids which are usually used in practical systems, for example in SpaceEx [Frehse et al. (2011)] and Ellipsoid Toolbox [Kurzanskiy and Varaiya (2006)], a more precise transformed safety specification can be derived by our element to element approach in Section 3 since $\delta_i \leq \|\delta\|$, thus it performs better than the δ -neighborhood approach.

In the following, we present detailed algorithms to transform the safety specifications described by convex polytopes and ellipsoids.

4.1 Transforming Safety Specifications

4.1.1 $S(M_n)$ as Convex Polytopes

Assume that the safety specification of the full-order system is of the form:

$$S(M_n) = \{y \in \mathbb{R}^p \mid \Gamma y + \Psi \leq 0\}, \quad (5)$$

where $\Gamma = [\alpha_{ij}] \in \mathbb{R}^{q \times p}$ and $\Psi = [\beta_i] \in \mathbb{R}^q$.

Lemma 2 *Given $S(M_n)$ described by (5), then $S(M_k^\delta)$ and $U(M_k^\delta)$ defined as follows guarantee the safety relation (1).*

$$\begin{aligned} S(M_k^\delta) &= \{y_r \in \mathbb{R}^p \mid \Gamma y_r + \bar{\Psi} \leq 0\}, \\ U(M_k^\delta) &= \{y_r \in \mathbb{R}^p \mid \Gamma y_r + \underline{\Psi} > 0\}, \\ \bar{\Psi} &= \Psi + \Delta, \quad \underline{\Psi} = \Psi - \Delta, \\ \Delta &= [\Delta_i] \in \mathbb{R}^q, \quad \Delta_i = \sum_{j=1}^p |\alpha_{ij}| \delta_j. \end{aligned} \quad (6)$$

The proof is given in Appendix 8.1.

4.1.2 $S(M_n)$ as Ellipsoids

Assume that the safety specification of the full-order system is described by an ellipsoid with radius R as:

$$S(M_n) = \{y \in \mathbb{R}^p \mid (y - a)^T Q (y - a) \leq R^2\}, \quad (7)$$

where a is the center of the ellipsoid and $Q \in \mathbb{R}^{p \times p}$ is a symmetric positive definite matrix.

Since Q is a symmetric matrix, there exists an orthogonal matrix $E = [l_1, l_2, \dots, l_p] = [\gamma_{ij}] \in \mathbb{R}^{p \times p}$ such that $E^T Q E = \Lambda = \text{diag}(\lambda_1, \lambda_2, \dots, \lambda_p)$, where $\lambda_i (> 0)$ is eigenvalue of Q and l_i is the eigenvector of Q corresponding to λ_i . The transformed safety and unsafe specifications of the output abstraction can be obtained with the following lemma.

Lemma 3 *Given $S(M_n)$ described by (7), then $S(M_k^\delta)$ and $U(M_k^\delta)$ defined as follows guarantee the safety relation (1):*

$$\begin{aligned} S(M_k^\delta) &= \{y_r \in \mathbb{R}^p \mid (y_r - a)^T Q (y_r - a) \leq (R - \Delta_R)^2\}, \\ U(M_k^\delta) &= \{y_r \in \mathbb{R}^p \mid (y_r - a)^T Q (y_r - a) > (R + \Delta_R)^2\}, \\ \Delta_R &= \sqrt{\sum_{i=1}^p [\lambda_i (\sum_{j=1}^p |\gamma_{ij}| \delta_j)^2]}. \end{aligned}$$

The proof of this result is given in Appendix 8.1.

We can see that the transformed safety specification of the output abstraction is also an ellipsoid (with smaller radius $R - \Delta_R$) located inside the original ellipse defining the safety specification of the full-order system. Meanwhile the corresponding transformed unsafe specification is defined by the region outside the larger ellipse with the radius $R + \Delta_R$.

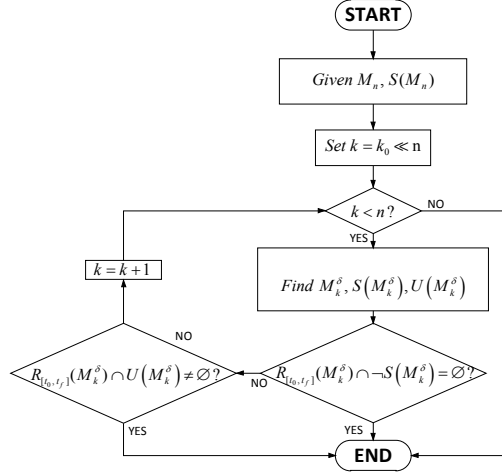


Fig. 1: Semi-algorithm for automatic safety verification using output abstraction.

4.1.3 Further discussion

Lemmas 2 and 3 can be applied directly for the system with bounded safety specification (i.e., the safety specification is bounded and thus, the unsafe specification is unbounded). Conversely, it is easy to see that our method can also be applied for the system with unbounded safety specification (i.e., the unsafe specification is bounded). Assume that the unsafe specification of the full-order system is bounded by a convex polytope as follows:

$$U(M_n) = \{y \in \mathbb{R}^p \mid \Gamma y + \Psi \leq 0\}, \quad (8)$$

where Γ and Ψ are defined as in (5). Then, the transformed unsafe specification for the output abstraction is defined by:

$$U(M_k^\delta) = \{y_r \in \mathbb{R}^p \mid \Gamma y_r + \underline{\Psi} \leq 0\}, \quad (9)$$

where $\underline{\Psi}$, Δ are defined as in Lemma 2.

Similarly, suppose the unsafe specification of the full-order system is bounded by an ellipsoid with radius R :

$$U(M_n) = \{y \in \mathbb{R}^p \mid (y - a)^T Q (y - a) \leq R^2\}, \quad (10)$$

where a and Q are defined as in (7). Then, the corresponding transformed unsafe specification for the output abstraction is bounded by the following:

$$U(M_k^\delta) = \{y_r \in \mathbb{R}^p \mid (y_r - a)^T Q (y_r - a) \leq (R + \Delta_R)^2\}, \quad (11)$$

where Δ_R is the same as in Lemma 3.

The proof for the above transformation is the same as in Lemmas 2 and 3. Geometrically, the transformed unsafe specification of the output abstraction is a larger region containing the unsafe region of the full-order system.

4.2 Safety Verification with Output Abstraction

Lemma 4 *Given a asymptotic stable LTI system M_n , whenever its output abstraction M_k^δ is safe or unsafe, it is sound to claim that the system M_n is safe or unsafe respectively.*

Proof According to Lemma 1, for a stable LTI system, there exists an output abstraction M_k^δ . From the definition of the output abstraction, we can see that, for any output trajectory of M_n , there exists a corresponding output trajectory of M_k^δ such that the distance between two trajectories is always bounded by a sound $\|\delta\|$. Moreover from Lemmas 2 and 3, because the transformed specifications ($S(M_k^\delta)$ and $U(M_k^\delta)$) satisfy the safety relation (1), thus when each output trajectory of M_k^δ satisfies the transformed safety specification $S(M_k^\delta)$, its corresponding output trajectory of M_n also satisfies the original safety specification $S(M_n)$. That means, if all output trajectories of M_k^δ satisfy the transformed safety specification $S(M_k^\delta)$, then all output trajectories of M_n also satisfy the original safety specification $S(M_n)$. Consequently, when the output abstraction is safe, it is sound to claim that the full-order system is safe. A similar proof can be given for the unsafe case. The proof is completed.

So far, the process of obtaining an output abstraction and its safety specifications from a given high-dimensional linear system and safety requirements can be done automatically. A semi-algorithm for automatic safety verification of a high-dimensional system using its output abstraction is depicted in Figure 1. The method finds a k -dimension output abstraction ($k = k_0$ initially, where k_0 is given by the user) and the corresponding safety specification, then checks the safety of the output abstraction. The method may not terminate as checking the safety of the output abstraction is undecidable since it involves computing the reachable states for a linear system, so it is a semi-algorithm. However, in practice, tools such as SpaceEx may terminate for time-bounded overapproximate reachability computations for systems of small enough dimensionality.¹ If it is safe (or unsafe) then the method stops with the conclusion that the full-order system is safe (or unsafe) and returns the current k -order abstraction. If the safety of the output abstraction cannot be verified (i.e., it is indeterminate), then the algorithm will repeat the same process for another output abstraction whom the order is increased by 1 from the order of the current abstraction.

We have discussed how to use an output abstraction for verification and proposed an semi-algorithm to obtain automatically an appropriate output abstraction. In the next section, the method is extended to a class of periodically switched linear systems.

5 Output Abstraction and Verification for Periodically Switched Systems

In this section, we extend our previous results to verify the safety of periodically switched systems (PSSs).

¹ Note that we cannot use SpaceEx to conclude a system is unsafe because it computes over-approximations of the actual set of reachable states. We could conclude unsafety if under-approximations were available, but not many tools compute under-approximations.

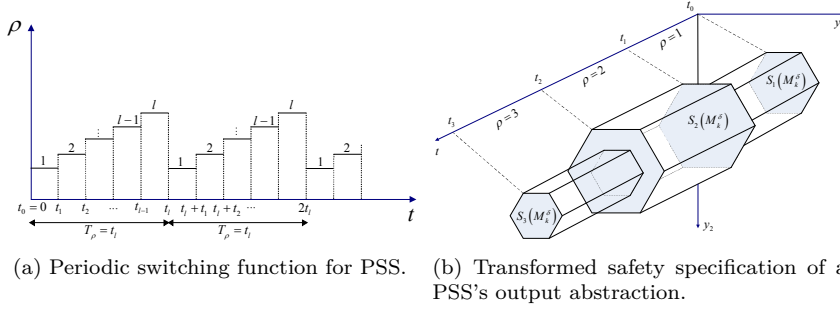


Fig. 2

5.1 Output Abstraction for Periodically Switched Systems

To define the class of PSSs, we need to define the notion of periodical switching signal $\rho(t)$.

Let $\mathcal{P} = \{1, 2, \dots, l-1, l\}$, where $l \in \mathbb{N}$ and $\mathcal{T} = \{t_0, t_1, t_2, \dots, t_{l-1}, t_l\}$. The periodical piecewise constant function $\rho(t)$ describing the switching signal is assumed to be right-continuous everywhere and is defined by:

$$\begin{cases} \rho(t) = i, & t_{i-1} \leq t < t_i, \quad i \in \mathcal{P} \\ \rho(k \times t_l + t) = \rho(t), & t_0 \leq t < t_l, \quad k = 0, 1, 2, \dots \end{cases}$$

Figure 2a illustrates a periodic switching function with the assumption that $t_0 = 0$. For simplicity, we omit the time argument of switching function in the rest of the paper. The class of PSS is given by:

$$\begin{aligned} \dot{x}(t) &= A_\rho x(t) + B_\rho u(t), \quad t \notin \mathcal{T}, \\ x(t^+) &= r_\rho(x(t)), \quad t \in \mathcal{T}, \quad x(t^+) \in X_\rho^o \\ y(t) &= C_\rho x(t), \end{aligned} \tag{12}$$

where $x(t) \in \mathbb{R}^n$ is the system state, $y(t) \in \mathbb{R}^p$ is the system output, $u(t) \in \mathbb{R}^m$ is the control input, and (A_ρ, B_ρ, C_ρ) are system matrices in the “mode” ρ ; $r_\rho(\cdot)$, and X_ρ^o respectively are the bounded resetting function and the initial set of state in the “mode” ρ . In particular, the first equation of (12) describes the continuous dynamics of the PSS and the second equation represents the resetting law. For brevity, we denote M_n as the full-order PSS defined by (12).

The above class of switched systems with resetting functions can be found in some supervisory control structures with the employment of impulsive control techniques. Once the system state is observed to reach some unsafe large values far away from initial set, some impulsive control schemes can be activated to abruptly drag the state back to the initial set to ensure the safety of the system. Note that in this paper, the resetting functions are activated periodically along with time (i.e., they do not depend on state variables).

Since the initial state for each mode is specified in each switching time, using the same approach as for linear continuous system, we can find the reduced-order representation called the local output abstraction for each mode of M_n that produces the output signal capturing the full-order system output signal within an computable

error bound. In other words, we can derive the output abstraction M_k^δ for the full-order PSS M_n as:

$$\begin{aligned} \dot{x}_r(t) &= \check{A}_\rho x_r(t) + \check{B}_\rho u(t), \quad t \notin \mathcal{T}, \\ x_r(t^+) &= S T_\rho x(t^+), \quad t \in \mathcal{T} \\ y_r(t) &= \check{C}_\rho x_r(t), \end{aligned} \tag{13}$$

where $x_r(t) \in \mathbb{R}^k$, $y_r(t) \in \mathbb{R}^p$ and the system matrices $(\check{A}_\rho, \check{B}_\rho, \check{C}_\rho)$ of the abstraction in mode ρ can be obtained using the balanced truncation reduction method Section 3 defined by the balancing transformation matrix T_ρ and the cutting matrix $S = \begin{pmatrix} I_{k \times k} & 0_{k \times (n-k)} \end{pmatrix}$.

The output signal of the abstraction M_k^δ captures the output of the full-order system M_n at all the times t within a piecewise linear constant error bound $\delta_\rho = [\delta_1^\rho, \delta_2^\rho, \dots, \delta_p^\rho]^T$ which can be computed in the same manner as in the case of linear continuous systems in Section 3.

This summarizes the procedure for deriving the output abstraction for the full-order PSS. Next, we consider how to use the output abstraction to verify safety of the full-order PSS.

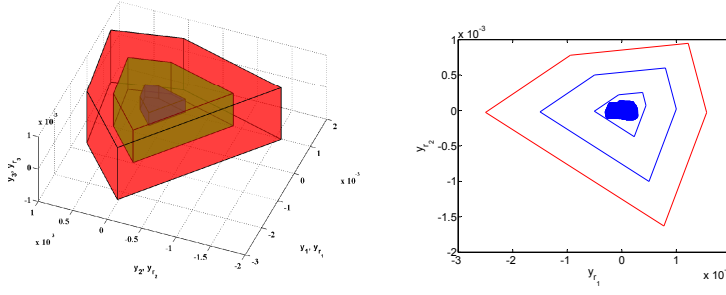
5.2 Verification for Periodically Switched Systems

Similar to the case of linear continuous system, the key step for the verification process is that from the computed error bound δ_ρ and the given safety specification of the full-order PSS system, we determine the safety specifications for the corresponding output abstraction that guarantees the safety relation (1).

Let us consider the first case that the safety specification of the full-order PSS (12) is described by (5) (i.e. as a polytope). The transformed safety specifications for the corresponding output abstraction (13) that satisfies the safety relation (1) is defined by:

$$\begin{aligned} S(M_k^\delta) &= \bigcup_{\rho} S_\rho(M_k^\delta), \quad U(M_k^\delta) = \bigcup_{\rho} U_\rho(M_k^\delta), \\ S_\rho(M_k^\delta) &= \{y_r \in \mathbb{R}^p \mid \Gamma y_r + \bar{\Psi}^\rho \leq 0\}, \\ U_\rho(M_k^\delta) &= \{y_r \in \mathbb{R}^p \mid \Gamma y_r + \underline{\Psi}^\rho > 0\}, \\ \bar{\Psi}^\rho &= \Psi + \Delta_\rho, \quad \underline{\Psi}^\rho = \Psi - \Delta_\rho, \\ \Delta_\rho &= [\Delta_i^\rho] \in \mathbb{R}^q, \quad \Delta_i^\rho = \sum_{j=1}^p |\alpha_{ij}| \delta_j^\rho. \end{aligned}$$

Similarly, when the safety specification of the full-order PSS has the form of an ellipsoid as defined in (7), we can derive the corresponding transformed safety specification for the output abstraction as follows.



(a) Safety specification S_{270} of the full order ISS system which is the region inside the middle green polytopes and the transformed safety specifications of its 10-order output abstraction in which the safe region S_{10}^δ is inside the smallest blue polytopes and the unsafe region U_{10}^δ is outside the largest red polytopes.

(b) Reachable set of (y_{r1}, y_{r2}) of the ISS's 10-order abstraction M_{10}^δ in the period of time $[0, 20s]$ and its safe region S_{12}^δ (inside the smallest blue polygon) and unsafe region U_{12}^δ (outside the red polygon).

Fig. 3

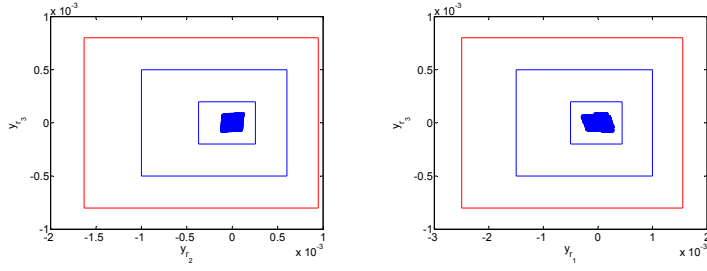
$$\begin{aligned}
 S(M_k^\delta) &= \bigcup_{\rho} S_{\rho}(M_k^\delta), \quad U(M_k^\delta) = \bigcup_{\rho} U_{\rho}(M_k^\delta), \\
 S_{\rho}(M_k^\delta) &= \{y_r \in \mathbb{R}^p \mid (y_r - a)^T Q (y_r - a) \leq (R - \Delta_R^\rho)^2\}, \\
 U_{\rho}(M_k^\delta) &= \{y_r \in \mathbb{R}^p \mid (y_r - a)^T Q (y_r - a) > (R + \Delta_R^\rho)^2\}, \\
 \Delta_R^\rho &= \sqrt{\sum_{i=1}^p [\lambda_i (\sum_{j=1}^p |\gamma_{ij}| \delta_j^\rho)^2]}.
 \end{aligned}$$

We have obtained the transformed safety specification for the output abstraction of a PSS. Since the error bound δ_ρ varies along with time (i.e. it depends on what mode is being activated), the transformed safety specification for the output abstraction also varies along with time. In addition, it is periodic because of the periodicity of the switching function $\rho(t)$. Figure 2b presents an example of the transformed safety specification of a PSS with two outputs. From the transformed safety specification, we can verify straightforwardly the safeness of the output abstraction to conclude about safety of its full-order PSS.

We have considered how to obtain an output abstraction and use it to verify safety of PSS. In the next section, several case of studies are presented to evaluate the benefits of our method.

6 Case Studies and Evaluation

To evaluate the order-reduction abstraction method presented in this paper, we implemented a software prototype that automatically creates output abstractions from full-order systems and applied it to a set of benchmarks. The method is integrated



(a) Reachable set of (y_{r2}, y_{r3}) of the ISS's 10-order abstraction M_{10}^o in the period of time $[0, 20s]$ and its safe region S_{23}^δ (inside the smallest blue polygon) and unsafe region U_{23}^δ (outside the red polygon).
 (b) Reachable set of (y_{r1}, y_{r3}) of the ISS's 10-order abstraction M_{10}^o in the period of time $[0, 20s]$ and its safe region S_{13}^δ (inside the smallest blue polygon) and unsafe region U_{13}^δ (outside the red polygon).

Fig. 4

in HyST by calling Matlab related functions.² In this section, we first evaluate the advantages and disadvantages of our method in computing the error bound and its performance. Our results are compared with the results produced by the approximate bisimulation relations method [Girard and Pappas (2007a)] and the simulation-based approach [Han and Krogh (2004)] via several benchmarks presented in Table 2. Then, we consider in detail how to apply our method to verify the safety of two specific case studies.

Error bound and computation time evaluation. The experiments are using Matlab 2014a and SpaceEx on a personal computer with the following configuration: Intel (R) Core(TM) i7-2677M CPU at 1.80GHz, 4GB RAM, and 64-bit Window 7. We set the upper limit for Matlab simulation and SpaceEx running time as two hours. It is said to be out of time (OOT) if we can not get the result after two hours.

Table 4 presents the error bounds and computation times of different methods on some typical benchmarks. The approximate bisimulation method proposed in [Girard and Pappas (2007a)] is integrated in the Matlab toolbox called MATISSE. The simulation-based method proposed in [Han and Krogh (2004)] is done automatically in this paper. The results of our method are presented separately as follows. In the

² The prototype implementation and SpaceEx model files for the examples evaluated, both before and after order reduction, are available at: <http://verivital.com/hyst/pass-order-reduction/>.

No.	Benchmark	Type	n	m	p
1	Motor control system (MCS)	LTI	8	2	2
2	Helicopter [Frehse et al. (2011)]	LTI	28	6	2
3	Building model (BM) [Chahlaoui and Van Dooren (2002)]	LTI	48	1	1
4	International space station (ISS) [Chahlaoui and Van Dooren (2002)]	LTI	270	3	3
5	Partial differential equation (Pde) [Chahlaoui and Van Dooren (2002)]	LTI	84	1	1
6	FOM [Chahlaoui and Van Dooren (2002)]	LTI	1006	1	1
7	Synchronous position control system with 2 motors (SMS2)	PSS	8	2	2

Table 2: Benchmarks for the order-reduction abstraction method in which n is dimension of the system; m and p are the number of inputs and outputs respectively.

first part named “Mixed bound”, we compute the bound of e_1 using Theorem 2 and the bound of e_2 using simulation. In the second part named “Theoretical bound”, the bounds of e_1 and e_2 are computed using Theorem 1 and Theorem 3 respectively. We remind that, for p -output MIMO system, the simulation-based method and our proposed method compute separately the error bound for each pair of output (i.e. $\|y^i - y_r^i\|$, $1 \leq i \leq p$) while the approximate bisimulation method computes the total error bound (i.e. $\|y - y_r\|$).

Let us consider the bound of e_1 related to the initial set of states X_0 that is computed using the two different techniques proposed in this paper. For the helicopter and partial differential equation benchmarks, the initial set of states X_0 is far from the zero point. The bounds of e_1 computed using Theorem 1 is large and too conservative which may not be useful. For the motor control system and building model benchmarks, the initial set of states X_0 is close to the zero point. The bounds of e_1 computed by Theorem 1 are fairly good and acceptable. We can see that the bounds of e_1 computed using Theorem 2 is much smaller than the ones computed by Theorem 1 for any situation of X_0 .

Now, we analyze the bound of e_2 computed by Theorem 3 where the effect of Hankel singular values on this bound as mentioned in Remark 1 can be illustrated. For the PDE benchmark, it can be seen that the theoretical bounds of e_2 for all cases of the output abstraction’s dimension k are very small due to the fact that the Hankel singular values σ_k (which are not presented here) of the corresponding balanced system are very small (almost equal to zero) as $k \geq 5$. We can see more clearly the effect of these Hankel singular values by looking at the helicopter benchmark. The theoretical bound of e_2 becomes larger when the lower dimension output abstraction is obtained. It is small as k equal to 20 because $\sum_{21}^{28} \sigma_j$ is small. The theoretical bound of e_2 becomes conservative as $k = 10$ since $\sum_{11}^{28} \sigma_j$ is large. It can be shown that the bound of e_2 computed using simulation method is much less conservative than the theoretical bound. Although Theorem 3 may give conservative result for some systems, it is still useful for some other systems as analyzed above. The benefit

Benchmark	Initial set of states $X_0 = \{x_0 \in \mathbb{R}^n \mid lb(i) \leq x_0(i) \leq ub(i), 1 \leq i \leq n\}$	Input constraint $u = [u_1, \dots, u_m]^T$	Safety specification $y = [y_1, \dots, y_p]^T$
Motor control system	$lb(i) = ub(i) = 0, i = 2, 3, 4, 6, 7, 8,$ $lb(2) = 0.002, ub(2) = 0.0025,$ $lb(3) = 0.001, ub(3) = 0.0015.$	$u_1 \in [0.16, 0.3],$ $u_2 \in [0.2, 0.4].$	unsafe region: $0.35 \leq y_1 \leq 0.4,$ $0.45 \leq y_2 \leq 0.6.$
Helicopter	$lb(i) = ub(i) = 0.1, i = 1, 4, 5, 6, 7,$ $lb(2) = lb(3) = 0.098, ub(2) = 0.11, ub(3) = 0.102,$ $lb(i) = ub(i) = 0, 8 \leq i \leq 28.$	$u_i \in [-1, 1],$ $1 \leq i \leq 6.$	unsafe region: $-1 \leq y_1 \leq 1,$ $10 \leq y_2$
Building model	$lb(i) = 0.0002, ub(i) = 0.00025, 1 \leq i \leq 10,$ $lb(25) = -0.0001, ub(25) = 0.0001,$ $lb(i) = ub(i) = 0, 11 \leq i \leq 48, i \neq 25.$	$u_1 \in [0.8, 1].$	unsafe region: $0.008 \leq y_1$
Partial differential equation	$lb(i) = 0, ub(i) = 0, 1 \leq i \leq 64$ $lb(i) = 0.001, ub(i) = 0.0015, 64 \leq i \leq 80,$ $lb(i) = -0.002, ub(i) = -0.0015, 81 \leq i \leq 84.$	$u_1 \in [0.5, 1].$	safe region: $y_1 \leq 12$
International space station	$lb(i) = -0.0001, ub(i) = 0.0001, 1 \leq i \leq 270.$	$u_1 \in [0, 0.1],$ $u_2 \in [0.8, 1],$ $u_3 \in [0.9, 1].$	Safe region: $-461y_1 + 887y_2 + 0.67 \leq 0,$ $-440y_1 - 898y_2 - 0.68 \leq 0,$ $-76.7y_1 + 997y_2 - 0.54 \leq 0,$ $898y_1 - 440y_2 - 0.89 \leq 0,$ $945y_1 + 326y_2 - 0.95 \leq 0,$ $-0.0005 \leq y_3 \leq 0.0005.$
FOM	$lb(i) = -0.0001, ub(i) = 0.0001, 1 \leq i \leq 400$ $lb(i) = 0.0002, ub(i) = 0.00025, 401 \leq i \leq 800,$ $lb(i) = 0, ub(i) = 0, 801 \leq i \leq 1006.$	$u_1 \in [-1, 1].$	safe region: $y_1 \leq 45$

Table 3: Initial states, input constraints and safety specification of LTI benchmarks.

Benchmark	k	[Girard and Pappas (2007a)]		[Han and Krogh (2004)]		Mixed bound				Theoretical bound			
		δ	$t(s)$	δ	$t(s)$	e_1	e_2	δ	$t(s)$	e_1	e_2	δ	$t(s)$
Motor control system	5	2.1	0.93	$\begin{pmatrix} 0.0021 \\ 0.047 \end{pmatrix}$	0.17	$2^2 + 2$	$\begin{pmatrix} 0.00049 \\ 0.00062 \end{pmatrix}$	$\begin{pmatrix} 0.002 \\ 0.047 \end{pmatrix}$	0.92	$\begin{pmatrix} 0.0098 \\ 0.0093 \end{pmatrix}$	$\begin{pmatrix} 0.53 \\ 0.53 \end{pmatrix}$	$\begin{pmatrix} 0.54 \\ 0.54 \end{pmatrix}$	0.15
	4	1.5	0.64	$\begin{pmatrix} 0.036 \\ 0.047 \end{pmatrix}$	0.19	$2^2 + 2$	$\begin{pmatrix} 0.00086 \\ 0.00062 \end{pmatrix}$	$\begin{pmatrix} 0.035 \\ 0.047 \end{pmatrix}$	0.9	$\begin{pmatrix} 0.009 \\ 0.009 \end{pmatrix}$	$\begin{pmatrix} 0.91 \\ 0.91 \end{pmatrix}$	$\begin{pmatrix} 0.92 \\ 0.92 \end{pmatrix}$	0.15
Helicopter	20	0.84	17	$\begin{pmatrix} 7.1e-05 \\ 4.3e-05 \end{pmatrix}$	0.6	$2^4 + 6$	$\begin{pmatrix} 0.0072 \\ 0.018 \end{pmatrix}$	$\begin{pmatrix} 5.7e-05 \\ 3.2e-05 \end{pmatrix}$	35	$\begin{pmatrix} 0.28 \\ 0.95 \end{pmatrix}$	$\begin{pmatrix} 0.0017 \\ 0.0017 \end{pmatrix}$	$\begin{pmatrix} 0.28 \\ 0.95 \end{pmatrix}$	0.49
	16	28	12	$\begin{pmatrix} 0.00075 \\ 0.0013 \end{pmatrix}$	0.56	$2^4 + 6$	$\begin{pmatrix} 0.0072 \\ 0.018 \end{pmatrix}$	$\begin{pmatrix} 0.0007 \\ 0.00087 \end{pmatrix}$	23	$\begin{pmatrix} 0.28 \\ 0.95 \end{pmatrix}$	$\begin{pmatrix} 0.029 \\ 0.029 \end{pmatrix}$	$\begin{pmatrix} 0.3 \\ 0.97 \end{pmatrix}$	0.45
	10	160	8.1	$\begin{pmatrix} 0.024 \\ 0.038 \end{pmatrix}$	0.55	$2^4 + 6$	$\begin{pmatrix} 0.0085 \\ 0.021 \end{pmatrix}$	$\begin{pmatrix} 0.021 \\ 0.031 \end{pmatrix}$	13	$\begin{pmatrix} 0.29 \\ 0.93 \end{pmatrix}$	$\begin{pmatrix} 1 \\ 1 \end{pmatrix}$	$\begin{pmatrix} 1.3 \\ 1.9 \end{pmatrix}$	0.45
	25	0.0096	180	0.0051	22	$2^{11} + 1$	0.013	$6.2e-05$	0.013	130	0.083	0.0072	0.09
Building model	15	0.069	120	0.005	18	$2^{11} + 1$	0.012	0.00044	0.013	58	0.078	0.084	0.16
	6	0.1	44	0.0058	14	$2^{11} + 1$	0.011	0.00025	0.012	24	0.073	0.21	0.28
Partial differential equation	30	0.75	230	N/A	OOT	$2^{20} + 1$	0.033	$5.6e-14$	0.033	1500	1	$5e-12$	1
	20	0.038	160	N/A	OOT	$2^{20} + 1$	0.033	$3.5e-14$	0.033	890	1	$5.4e-12$	1
	10	0.086	55	N/A	OOT	$2^{20} + 1$	0.033	$9.8e-13$	0.033	520	0.92	$2.7e-11$	0.92
	6	0.1	42	N/A	OOT	$2^{20} + 1$	0.033	$3.5e-07$	0.033	370	0.89	$5.6e-06$	0.89
International space station	25	N/A	OOT	N/A	OOT	$2^{270} + 3$	N/A	$\begin{pmatrix} 2.1e-05 \\ 0.001 \\ 4.6e-05 \end{pmatrix}$	N/A	OOT	$\begin{pmatrix} 0.00043 \\ 0.00026 \\ 0.00026 \end{pmatrix}$	$\begin{pmatrix} 0.47 \\ 0.47 \\ 0.47 \end{pmatrix}$	11
	10	N/A	OOT	N/A	OOT	$2^{270} + 3$	N/A	$\begin{pmatrix} 2.4e-05 \\ 5.6e-05 \\ 9e-05 \end{pmatrix}$	N/A	OOT	$\begin{pmatrix} 0.00042 \\ 0.00022 \\ 0.00021 \end{pmatrix}$	$\begin{pmatrix} 1.7 \\ 1.7 \\ 1.7 \end{pmatrix}$	12
FOM model	20	N/A	OOT	N/A	OOT	$2^{800} + 1$	N/A	$2.7e-07$	N/A	OOT	1.3	$1.1e-05$	1.3
	15	N/A	OOT	N/A	OOT	$2^{800} + 1$	N/A	0.00021	N/A	OOT	1.3	0.0065	1.3
	10	N/A	OOT	N/A	OOT	$2^{800} + 1$	N/A	0.1	N/A	OOT	1.3	2.2	3.5

Table 4: The error bounds and computation times obtained from different methods on different benchmarks in which: k is the dimension of the output abstraction, δ is total error bound, e_1 is the zero input response error, e_2 is the zero state response error, t is the error computing time (in second) and N is the number of simulations. The terms of “N/A” and “OOT” mean “not applicable” and “out of time”, respectively.

Benchmark	Full Order System		Output Abstraction			
	Time(s)	Memory(Kb)	k	$T_1(s)$	$T_2(s)$	Total time(s)
Motor control system	27	3048	5	26	0.92	26.9
			4	16.7	0.9	17.6
			20	206	35	241
Helicopter	287	3052	16	128	23	151
			10	68	13	81
			25	237.2	130	367.2
Building model	893	3056	15	82.3	58	140.3
			6	19.5	24	43.5
			30	725.6	1500	2225.6
Partial differential equation	OOT	N/A	20	310	890	1200
			10	75.2	520	595.2
			6	31.9	370	401.9
			25	254.3	11	265.3
International space station	OOT	N/A	10	72.8	12	84.8
			20	95.4	48	143.4
FOM model	OOT	N/A	15	56.2	48	104.2
			10	34.8	48	82.8
			20	95.4	48	143.4

Table 5: Computation cost for verification process of the full order original LTI system and its output abstractions using SpaceEx [Frehse et al. (2011)] in which T_1 is the time for SpaceEx to compute the reach set of the output abstraction; T_2 is the time for obtaining the output abstraction; “Total Time” column states for the total time of verification process for the output abstraction, “Memory” column presents the memory used for computing reach set which is measure in kilobyte; time is measured in second. The terms of “N/A” and “OOT” mean “not applicable” and “out of time”.

of the theoretical bound is we can calculate the bound very quickly without doing simulation and thus avoid the numerical issues in simulation-based methods.

We have discussed the benefits and drawbacks of different techniques proposed in this paper. Now, we make a short comparison with the approximate bisimulation relation method [Girard and Pappas (2007a)] and simulation-based method [Han and Krogh (2004)]. As can be seen from Table 4, the simulation-based approach gives very tight bounds for the errors (for examples, the motor control system and heli-

copter benchmarks). This approach is powerful when dealing with systems having small number of vertices in the initial set. When the number of vertices increases, the number of simulations also grows exponentially as can be seen from Table 4. Therefore, it is difficult to apply the simulation-based approach in this situation (e.g. PDE, ISS and FOM benchmarks). For the approximate bisimulation relation method (integrated in Matisse toolbox), it can be observed that for PDE benchmark, this approach can give a good error bound. However, for MCS and Helicopter benchmarks, this approach gives very conservative results (which may not be useful) due to the appearance of ill-conditioned matrices in the process of solving LMI and optimization problems. We can see that for all the benchmarks on which the approximate bisimulation relation method can be applied, combination of using Theorem 2 and simulation bound of e_2 (i.e. mixed bound) produces much less conservative error bounds. When the dimension of the system is large (e.g. as in the ISS and FOM benchmarks), while the approximate bisimulation approach and Theorem 2 give no results due to running out of time, our theoretical approach can still be applied.

Toward the computation time of different methods, we can see from the table that our method using Theorem 1 and Theorem 3 has smallest computing time while using Theorem 2 and approximate bisimulation relation method require much more time to compute the error bound.

In summary, we can use different methods to compute the error bound between the full-order system and the output abstraction. Each method has benefits and drawbacks. The time complexity and the conservativeness of the result is a tradeoff that we need to take into account when applying these method to a specific system. As a suggestion from doing the experiment for this paper, for a system having dimension under 100, we can generally use Theorem 2, approximate bisimulation relation method [Girard and Pappas (2007a)] or simulation-based approach [Han and Krogh (2004)] to compute the error bound. For systems with more than 100 dimensions, we can use Theorem 1 and Theorem 3 or combine Theorem 1 (for determining e_1 bound) and simulation-based approach (for computing e_2 bound).

We have evaluated the error bounds and computation times of different methods. Next, we discuss about the benefit of using output abstraction for safety verification. Table 5 shows the computation cost of the verification process for the full-order LTI benchmarks and their different output abstractions. The bounded times for running all SpaceEx models are set as $t_f = 20s$. In the table, T_1 is the time for SpaceEx to compute the reach set of the output abstraction; T_2 is the time for obtaining the output abstraction; “Total Time” column states for the total time of verification process for the output abstraction, “Memory” column presents the memory used for computing reach set which is measure in kilobyte; all times are measure in second. For the first three systems (MCS, helicopter and BM), we combine Theorem 2 (for determining e_1 bound) and simulation-based approach (for computing e_2 bound) to derive the output abstraction. For the rest three benchmarks, we use Theorem 2 (for determining e_1 bound) and simulation-based approach (for computing e_2 bound) to obtain the output abstraction. As shown in the table, although using output abstraction does not help much to reduce the memory used in verification, it can help to reduce significantly the computation time. Moreover, output abstraction can be applied to check the safety of high-dimensional systems (e.g. PDE, ISS and FOM) that can not be verified directly using existing verification tools. Next, we consider the whole process of using output abstraction to verify the safety of two specific systems.

International Space Station (ISS). The full-order model (denoted by M_{270}) of the component $R1$ of the international space station has 270 state variables, three inputs and three outputs. We refer reader to [Antoulas et al. (2001)] for the state space model of the system, and it is also included in our supplementary materials. The initial condition, input constraints and safety specification of the ISS system are presented in Table 3.

Verification for the full-order system with 270 state variables may be difficult for existing verification tools. Output abstraction and safety specification transformation can help to verify safety of such high-dimensional system with a small computation cost. There are different output abstractions that can be used to verify whether the full-order system satisfies its safety requirements. In this paper, we use a 10-order output abstraction and the corresponding transformed safety specification to check the safety of the full-order system. From the safety requirement of the full-order system and the error bound shown in Table 4, we can see that the theoretical bound of e_2 is too conservative and cannot be used. To overcome this problem, we combine the theoretical bound of e_1 and the simulation bound of e_2 to derive a better bound between the full-order system and its 10-order output abstraction (denoted by M_{10}^δ). The error bound δ from this combination is $\delta = 10^{-3} \times [0.44, 0.28, 0.3]^T$.

The safety specification of the full-order ISS system S_{270} is visualized by the region inside the middle blue polytopes in Figure 3a. The transformed safety specifications (safe and unsafe specifications) of the corresponding 10-order output abstraction respectively are the region inside the smallest blue polytopes and the region outside the red polytopes.

Figures 3b, 4a and 4b present the safety specification transformation and output reach set in the period of time $[0, 20s]$ computed by SpaceEx [Frehse et al. (2011)] of the 10-order output abstraction on 2-dimension axes.

In the figures, the regions inside the middle blue polygons are the 2-dimensions projected safety regions of the full-order system. The corresponding projected transformed safety and unsafe specifications $S_{10}^\delta, U_{10}^\delta$ of the output abstraction are described by the regions inside the smallest blue polygons and the regions outside the red polygons respectively. The reach set $R_{ij}^\delta, i \neq j, 1 \leq i, j \leq 3$ for each pair output (y_{r_i}, y_{r_j}) of the abstraction M_{10}^δ are depicted by the solid blue regions. As shown in the figures, for all (i, j) , we have $R_{ij}^\delta \cap \neg S_{10}^\delta = \emptyset$, or in other words, $M_{10}^\delta \models S_{10}^\delta$, thus it can be concluded that the full-order system M_{270} satisfies the safety requirement S_{270} . Therefore, the full-order system is safe.

Periodically switched synchronous motor position control system. We have applied our method for safety verification of a high-dimensional LTI system above. Next, we consider how to use the proposed method to verify safety of a periodically switched synchronous motor system, which is used widely in many industrial fields such as elevator control systems, robotics and conveyer control systems. In this system, two motors are controlled synchronously and periodically in both directions (i.e. clockwise and counterclockwise) to keep their position distance remaining in a desired range.

Two motors have the same parameters with the motors used in Carnegie Mellon's undergraduate controls lab. Each motor has its own controller which is designed to guarantee that: (a) the overshoot of the output does not exceed 16%; (b) the settling time is less than 0.04s; (c) No steady-state error, even in the presence of a step disturbance input. The system denoted by M_8 is modeled as a PSS with two modes as depicted in Figure 5 in which two motors are controlled to rotate clockwise in

mode 1 and inversely in mode 2. The operating time in mode 1 is $t_1 = 0.1$ and the operating time in mode 2 is $t_2 = 0.15$.

The system's matrices in the two modes are given by:

$$A_0 = \begin{bmatrix} 0 & 1 & 0 & 0 \\ 0 & -1.0865 & 8487.2 & 0 \\ -2592.1 & -21.1190 & -698.9135 & -141390 \\ 1 & 0 & 0 & 0 \end{bmatrix},$$

$$B_0 = [0 \ 0 \ 0 \ -1]^T,$$

$$A_1 = A_2 = \begin{bmatrix} A_0 & 0 \\ 0 & A_0 \end{bmatrix}, B_1 = -B_2 = \begin{bmatrix} B_0 & 0 \\ 0 & B_0 \end{bmatrix},$$

$$C_1 = C_2 = \begin{bmatrix} 1 & 0 & 0 & 0 & 0 & 0 & 0 & 0 \\ 1 & 0 & 0 & 0 & -1 & 0 & 0 & 0 \end{bmatrix}.$$

The reference control input applied to the system is $u = [u_1 \ u_2]$, $0.16 \leq u_1 \leq 0.2$, $0.16 \leq u_2 \leq 0.22$. The initial set of states of the system in the two modes are defined by the hyperbox:

$$X_1^o = \{x \in \mathbb{R}^8 \mid lb_1^i \leq x(i) \leq ub_1^i, 1 \leq i \leq 8\},$$

$$X_2^o = \{x \in \mathbb{R}^8 \mid lb_2^i \leq x(i) \leq ub_2^i, 1 \leq i \leq 8\},$$

where (lb_1, ub_1) and (lb_2, ub_2) are initial conditions given in Table 6.

The first output of the system indicates the position of the first motor while the second output represents the position distance between the two motors. In order to make the system operate safely, the two motors are controlled synchronously so that the first motor position y_1 and the position error between the two motors y_2 do not reach unsafe regions defined by $U(M_8) = \{(y_1, y_2) \in \mathbb{R}^2 \mid 178(y_1 - 0.325)^2 + 625(y_2 - 0.16)^2 \leq 1, 178(y_1 + 0.325)^2 + 625(y_2 + 0.16)^2 \leq 1\}$. The unsafe regions of the full-order system are visualized by the regions inside the smallest red ellipses in Figure 6.

To verify safety of the full-order (8-dimensional) system, we use a 5th-order output abstraction M_5^δ and its transformed safety specification.

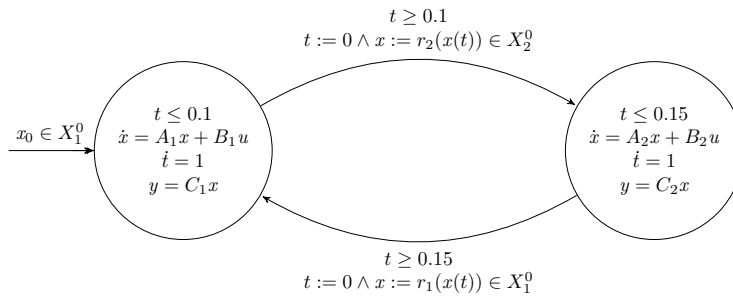


Fig. 5: Hybrid automaton model of the PSS synchronous motor control system.

Vector	Value
lb_1	$[-0.002 \ 0 \ 0 \ 0 \ -0.001 \ 0 \ 0 \ 0]^T$
ub_1	$[0.0025 \ 0 \ 0 \ 0 \ 0.002 \ 0 \ 0 \ 0]^T$
lb_2	$[-0.001 \ 0 \ 0 \ 0 \ -0.002 \ 0 \ 0 \ 0]^T$
ub_2	$[0.001 \ 0 \ 0 \ 0 \ 0.003 \ 0 \ 0 \ 0]^T$
lb_{r1}	$[-0.1373e-03 \ -0.5137e-03 \ -0.0586e-03 \ -0.2277e-03 \ -0.2235e-03]^T$
ub_{r1}	$[0.1323e-03 \ 0.5332e-03 \ 0.0930e-03 \ 0.3610e-03 \ 0.2320e-03]^T$
lb_{r2}	$[-0.1211e-03 \ -0.3684e-03 \ -0.0687e-03 \ -0.2666e-03 \ -0.1603e-03]^T$
ub_{r2}	$[0.0949e-03 \ 0.4703e-03 \ 0.0949e-03 \ 0.3684e-03 \ 0.2046e-03]^T$

Table 6: Initial condition vectors of synchronous motor control system and its 5th-order output abstraction.

The matrices for the output abstraction denoted in mode 1 and mode 2 respectively are:

$$\begin{aligned}
A_1^r &= A_2^r = \begin{bmatrix} -18.925 & 80.823 & 0 & 0 & -29.973 \\ -80.823 & -76.569 & 0 & 0 & 122.93 \\ 0 & 0 & -18.925 & -80.823 & 0 \\ 0 & 0 & 80.823 & -76.569 & 0 \\ -29.973 & -122.93 & 0 & 0 & -194.95 \end{bmatrix}, \\
B_1^r &= -B_2^r = \begin{bmatrix} 5.7806 & 7.3762 & 2.2080 & -2.8175 & 4.8964 \\ -3.5726 & -4.5587 & 3.5726 & -4.5587 & -3.0262 \end{bmatrix}^T, \\
C_1^r &= C_2^r = \begin{bmatrix} 3.5726 & -4.5587 & 3.5726 & 4.5587 & 3.0262 \\ 5.7806 & -7.3762 & -2.2080 & -2.8175 & 4.8964 \end{bmatrix}.
\end{aligned}$$

The transformed initial set of states the output abstraction in the two modes are defined by the hyperbox:

$$\begin{aligned}
\hat{X}_1^o &= \{x_r \in \mathbb{R}^5 \mid lb_{r1}^i \leq x_r^i \leq ub_{r1}^i, 1 \leq i \leq 5\}, \\
\hat{X}_2^o &= \{x_r \in \mathbb{R}^5 \mid lb_{r2}^i \leq x_r^i \leq ub_{r2}^i, 1 \leq i \leq 5\},
\end{aligned}$$

where (lb_{r1}^i, ub_{r1}^i) and (lb_{r2}^i, ub_{r2}^i) are given in Table 6.

We combine the optimization (for e_1 bound) and simulation (for e_2 bound) methods to determine the error bounds between the full-order system and its 5-order output abstraction. The error bounds in mode 1 and mode 2 respectively are $\delta_1 = [0.0234 \ 0.0189]^T$ and $\delta_2 = [0.0228 \ 0.0177]^T$. Using error bounds, the transformed unsafe specification for the output abstraction denoted by $U(M_5^\delta)$ is: $U(M_5^\delta) = \{(y_1, y_2) \in \mathbb{R} \mid 178(y_1 - 0.325)^2 + 625(y_2 - 0.16)^2 \leq 1.57^2, 178(y_1 + 0.325)^2 + 625(y_2 + 0.16)^2 \leq 1.57^2\}$. The unsafe regions for the output abstraction are the regions inside the largest red ellipsoids in Figure 6.

To ensure safety of the system, the output abstraction must not violate its transformed unsafe specification $U(M_5^\delta)$. From Figure 6, we can see that the output reach set of the output abstraction has an empty intersection with the unsafe regions, so we can conclude that the full-order system is safe.

7 Conclusion and Future Work

We have proposed an approach to verify safety specifications in high-dimensional linear systems and a class of periodically switched systems (PSSs) by verifying transformed safety specifications of a lower-dimensional output abstraction using existing

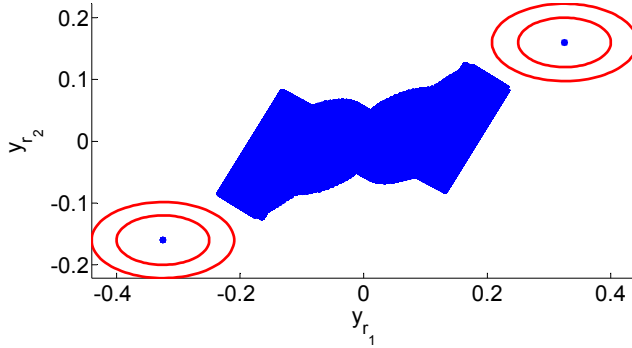


Fig. 6: Output reachable set in the period of time $[0, 20s]$ of the 5th-order output abstraction of the PSS synchronous motor position control system. The reach set does not reach the unsafe region (the region inside the largest red ellipse), thus the output abstraction is safe (with a bounded time interval), and thus the full-order system is safe (with a bounded time interval).

hybrid system verification tools. By reducing the dimensionality, our method significantly reduces the time and memory of reachability computations in the verification process.

There are several interesting directions for future work. First, the method for calculating the error bound corresponding to the zero input response (i.e. $\|e_1\|$) can only be used for stable LTI systems. Thus, a more general approach needs to be developed to deal with unstable linear systems. It is also important to find a general strategy to address the verification problem for high-dimensional nonlinear systems.

Additionally, our approach can be extended to more general hybrid systems. The main idea is that the states in each location that are related to guards/invariants need to be declared as the outputs of that location. Then, the output abstraction for each location can be obtained. A new hybrid system is then constructed based on these output abstractions. The guards/invariants of the new hybrid system are obtained by transforming the former guards/invariants of the original hybrid system in the same manner of safety specifications transformation proposed in this paper. This approach may benefit from other notions of “similarity” between behaviors (executions) of systems such as discrepancy functions [Duggirala et al. (2013)], or conformance degree [Abbas et al. (2014)].

References

Abbas, Haider, Hans Mittelmann, and Georgios Fainekos. 2014. Formal property verification in a conformance testing framework. In *Formal methods and models for codesign (memocode)*,

- 2014 twelfth acm/ieee international conference on, 155–164. IEEE. IEEE.
- Alur, Rajeev, Thomas Henzinger, Gerardo Lafferriere, George J Pappas, et al.. 2000. Discrete abstractions of hybrid systems. *Proceedings of the IEEE* 88 (7): 971–984.
- Antoulas, A. C., D. C. Sorensen, and S. Gugercin. 2001. A survey of model reduction methods for large-scale systems. *Contemporary Mathematics* 280: 193–219.
- Asarin, Eugene, and Thao Dang. 2004. Abstraction by projection and application to multi-affine systems. In *Hybrid systems: Computation and control*, 32–47. Springer.
- Bak, Stanley, Sergiy Bogomolov, and Taylor T. Johnson. 2015. HyST: A source transformation and translation tool for hybrid automaton models. In *18th international conference on hybrid systems: Computation and control* (hsccon 2015). Seattle, Washington: ACM.
- Belta, Calin, Volkan Isler, and George J Pappas. 2005. Discrete abstractions for robot motion planning and control in polygonal environments. *Robotics, IEEE Transactions on* 21 (5): 864–874.
- Chahlaoui, Younes, and Paul Van Dooren. 2002. A collection of benchmark examples for model reduction of linear time invariant dynamical systems..
- Chen, Xin, Erika Ábrahám, and Sriram Sankaranarayanan. 2013. Flow*: An analyzer for nonlinear hybrid systems. In *Computer aided verification*, 258–263. Springer. Springer.
- Danos, Vincent, and Cosimo Laneve. 2004. Formal molecular biology. *Theoretical Computer Science* 325 (1): 69–110.
- Duggirala, Parasara Sridhar, Sayan Mitra, and Mahesh Viswanathan. 2013. Verification of annotated models from executions. In *Proceedings of the eleventh acm international conference on embedded software. Emsoft '13*. Piscataway, NJ, USA: IEEE Press. ISBN 978-1-4799-1443-2.
- Frehse, Goran, Colas Le Guernic, Alexandre Donzé, Scott Cotton, Rajarshi Ray, Olivier Lebel-tel, Rodolfo Ripado, Antoine Girard, Thao Dang, and Oded Maler. 2011. Spaceex: Scalable verification of hybrid systems. In *Computer aided verification*, 379–395. Springer. Springer.
- Girard, Antoine, and George J Pappas. 2005. Approximate bisimulations for nonlinear dynamical systems. In *Decision and control, 2005 and 2005 european control conference. cdc-ecc'05. 44th ieee conference on*, 684–689. IEEE. IEEE.
- Girard, Antoine, and George J Pappas. 2007a. Approximate bisimulation relations for constrained linear systems. *Automatica* 43 (8): 1307–1317.
- Girard, Antoine, and George J Pappas. 2007b. Approximation metrics for discrete and continuous systems. *Automatic Control, IEEE Transactions on* 52 (5): 782–798.
- Girard, Antoine, A Agung Julius, and George J Pappas. 2008. Approximate simulation relations for hybrid systems. *Discrete Event Dynamic Systems* 18 (2): 163–179.
- Girard, Antoine, George J Pappas, et al.. 2006. Approximate bisimulation for a class of stochastic hybrid systems. In *American control conference, 2006*, 6. IEEE. IEEE.
- Han, Zhi. 2005. Formal verification of hybrid systems using model order reduction and decomposition. PhD diss, PhD thesis, Dept. of ECE, Carnegie Mellon University.
- Han, Zhi, and Bruce Krogh. 2004. Reachability analysis of hybrid control systems using reduced-order models. In *American control conference, 2004. proceedings of the 2004*, Vol. 2, 1183–1189. IEEE. IEEE.
- Han, Zhi, and Bruce H Krogh. 2006. Reachability analysis of large-scale affine systems using low-dimensional polytopes. In *Hybrid systems: Computation and control*, 287–301. Springer.
- Henzinger, Thomas A, and Joseph Sifakis. 2006. The embedded systems design challenge. In *Fm 2006: Formal methods*, 1–15. Springer.
- Islam, Md. Ariful, Abhishek Murthy, Ezio Bartocci, Elizabeth M. Cherry, Flavio H. Fenton, James Glimm, Scott A. Smolka, and Radu Grosu. 2015. Model-order reduction of ion channel dynamics using approximate bisimulation. *Theoretical Computer Science* 599: 34–46. doi:10.1016/j.tcs.2014.03.018. Advances in Computational Methods in Systems Biology.
- Julius, A Agung. 2006. Approximate abstraction of stochastic hybrid automata. In *Hybrid systems: Computation and control*, 318–332. Springer.
- Kong, Soonho, Sicun Gao, Wei Chen, and Edmund Clarke. 2015. dreach: δ -reachability analysis for hybrid systems.
- Kurzhanskiy, Alex A, and Pravin Varaiya. 2006. Ellipsoidal toolbox. *EECS Department, University of California, Berkeley, Tech. Rep. UCB/EECS-2006-46*.
- Moore, Bruce. 1981. Principal component analysis in linear systems: Controllability, observability, and model reduction. *Automatic Control, IEEE Transactions on* 26 (1): 17–32.

- Nesterov, Yurii, Arkadii Nemirovskii, and Yinyu Ye. 1994. *Interior-point polynomial algorithms in convex programming*, Vol. 13. SIAM.
- Obinata, Goro, and Brian DO Anderson. 2012. *Model reduction for control system design*. Springer.
- Pappas, George J. 2003. Bisimilar linear systems. *Automatica* 39 (12): 2035–2047.
- Regev, Aviv, Ekaterina M Panina, William Silverman, Luca Cardelli, and Ehud Shapiro. 2004. Bioambients: an abstraction for biological compartments. *Theoretical Computer Science* 325 (1): 141–167.
- Silverman, Leonard M, and HE Meadows. 1967. Controllability and observability in time-variable linear systems. *SIAM Journal on Control* 5 (1): 64–73.
- Tabuada, Paulo, and George J Pappas. 2004. Bisimilar control affine systems. *Systems & Control Letters* 52 (1): 49–58.
- Tanner, Herbert G, and George J Pappas. 2003. Abstractions of constrained linear systems. In *American control conference, 2003. proceedings of the 2003*, Vol. 4, 3381–3386. IEEE. IEEE.
- van der Schaft, Arjan. 2004. Equivalence of dynamical systems by bisimulation. *IEEE transactions on automatic control* 49 (12): 2160–2172.
- Vandenbergh, Lieven, and Stephen Boyd. 1994. Positive definite programming. *Mathematical Programming: State of the Art*.
- Wang, Yu, Nima Roohi, Matthew West, Mahesh Viswanathan, and Geir E. Dullerud. 2015. Statistical verification of dynamical systems using set oriented methods. In *Proceedings of the 18th international conference on hybrid systems: Computation and control. Hscc '15*, 169–178. New York, NY, USA: ACM. doi:10.1145/2728606.2728627. ISBN 978-1-4503-3433-4. <http://doi.acm.org/10.1145/2728606.2728627>.
- Ye, Yinyu, and Edison Tse. 1989. An extension of karmarkar's projective algorithm for convex quadratic programming. *Mathematical Programming* 44 (1-3): 157–179.

8 Appendix

8.1 Appendix: Proofs of Theorems

In this appendix, we present proofs of theorems presented in this paper.

8.1.1 Proof of Theorem 1

The basic idea of determining the theoretical bound of the first error e_1 relies on the concept of monotonic convergence defined as follows.

Definition 8 A homogeneous stable system $\dot{x} = Ax$ is called monotonic convergent if its states converge to zero and satisfy $\|x(t)\| \leq \|x(0)\|$, $\forall t \geq 0$.

Lemma 5 A homogeneous stable system $\dot{x} = Ax$ is a monotonic convergent system if $A + A^T < 0$.

Proof Choose the Lyapunov function $V(x(t)) = x(t)^T x(t)$, we have:

$$\dot{V}(x(t)) = x(t)^T (A + A^T) x(t) < 0.$$

Therefore, $V(x(t)) = \|x(t)\|^2 \leq V(x(0)) = \|x(0)\|^2$, $\forall t \geq 0$. This completes the proof.

Proof of Theorem 1:

We will show that the uncontrolled augmented system (i.e. $u = 0$) is a monotonic convergent system. To prove above statement, let consider the uncontrolled-balanced system: $\dot{\tilde{x}} = \tilde{A}\tilde{x}$. Since the system is balanced, we have:

$$\begin{aligned} \tilde{A}\Sigma + \Sigma\tilde{A}^T + BB^T &= 0 \\ \tilde{A}^T\Sigma + \Sigma\tilde{A} + C^TC &= 0. \end{aligned}$$

Combining two above equations yields:

$$(\tilde{A} + \tilde{A}^T)\Sigma + \Sigma(\tilde{A} + \tilde{A}^T) = -BB^T - C^TC.$$

It is easy to see that the real parts of all eigenvalues of $\tilde{A} + \tilde{A}^T$ are necessarily non-positive. Since $\tilde{A} + \tilde{A}^T$ is symmetric, it is non-positive. Note that \tilde{A} is asymptotically stable. Thus, using Lemma 5, we can conclude that the uncontrolled-balanced system is a monotonic convergent system.

Similarly, we can see that the uncontrolled-reduced system $\dot{x}_r = A_r x_r$ is also a monotonic convergent system. Since $\tilde{A} + \tilde{A}^T < 0$ and $A_r + A_r^T < 0$, we have $\tilde{A} + \tilde{A}^T < 0$, that means the uncontrolled augmented system is a monotonic convergent system.

Using the monotonic convergent property, the bound of the error e_1 satisfies:

$$\begin{aligned} \|e_1^i(t)\|^2 &= \|\bar{y}(i)\|^2 = \bar{x}^T \bar{C}_i^T \bar{C}_i \bar{x} \\ &\leq \lambda_{\max}(\bar{C}_i^T \bar{C}_i) \|\bar{x}\|^2 \\ &\leq \lambda_{\max}(\bar{C}_i^T \bar{C}_i) \|\bar{x}_0\|^2 \\ &\leq \lambda_{\max}(\bar{C}_i^T \bar{C}_i) \cdot \sup_{x_0 \in X_0} \|\bar{x}_0\|^2, \quad 1 \leq i \leq p. \end{aligned}$$

This completes the proof.

8.1.2 Proof of Theorem 2

Consider the uncontrolled augmented system (i.e. $u = 0$), let $V(\bar{x}(t)) = \bar{x}(t)^T P \bar{x}(t)$, we have $\dot{V}(\bar{x}(t)) = \bar{x}(t)^T (A^T P + P A) \bar{x}(t)$.

Assume P_0 is the solution of the optimization problem in Theorem 2. Because of $(A^T P_0 + P_0 A) < 0$, then $V(x(t)) < V(x(0)) = \bar{x}_0^T P_0 \bar{x}_0$. Note that $\|e_1^i(t)\|^2 = \bar{x}^T \bar{C}_i^T \bar{C}_i \bar{x}$, $1 \leq i \leq p$. Since we also have $\bar{C}_i^T \bar{C}_i \leq P_0$, the bound of the error satisfies $\|e_1^i(t)\| \leq \sqrt{\bar{x}_0^T P_0 \bar{x}_0}$.

This completes the proof.

8.1.3 Proof of Theorem 3

The theoretical bound of the second error e_2 can be derived straightforwardly using the concept of bounded input bounded output stability and the L_1 error bound in impulse response of balanced truncation model reduction [Obinata and Anderson (2012)]. From (3), we have:

$$\begin{aligned} |e_2(t)| &= |\tilde{y}_u - y_{r_u}| = \left| \int_0^t (\tilde{C} e^{\tilde{A}(t-\tau)} \tilde{B} - C_r e^{A_r(t-\tau)} B_r) u(\tau) d\tau \right| \\ &\leq \int_0^t |(\tilde{C} e^{\tilde{A}(t-\tau)} \tilde{B} - C_r e^{A_r(t-\tau)} B_r)| |u| d\tau \\ &\leq \|u\|_\infty \cdot \int_0^\infty |(\tilde{C} e^{\tilde{A}(t-\tau)} \tilde{B} - C_r e^{A_r(t-\tau)} B_r)| d\tau \\ &\leq \|u\|_\infty \cdot (2 \sum_{j=k+1}^n (2j-1) \sigma_j). \end{aligned}$$

Thus, $\|e_2^i(t)\| \leq \|u\|_\infty \cdot (2 \sum_{j=k+1}^n (2j-1) \sigma_j)$ which completes the proof.

8.1.4 Proof of Lemma 2

From the definition of output abstraction, we have:

$$\alpha_{ij} y_{r_j} - |\alpha_{ij}| \delta_j \leq \alpha_{ij} y_j \leq \alpha_{ij} y_{r_j} + |\alpha_{ij}| \delta_j.$$

$$\Rightarrow \Gamma y_r + \bar{\Psi}_2 \leq \Gamma y + \Psi \leq \Gamma y_r + \bar{\Psi}_1.$$

Thus, $S(M_k^\delta)$ and $U(M_k^\delta)$ defined by (6) satisfy the safety relation (1), which completes the proof.

8.1.5 Proof of Lemma 3

Let $\bar{y} = E(y - a)$, $\bar{y}_r = E(y_r - a)$. We have:

$$\begin{aligned} (y - a)^T Q (y - a) &= \bar{y}^T \Lambda \bar{y} = \sum_{i=1}^p \lambda_i \bar{y}_i^2, \\ (y_r - a)^T Q (y_r - a) &= \bar{y}_r^T \Lambda \bar{y}_r = \sum_{i=1}^p \lambda_i \bar{y}_{r_i}^2. \end{aligned} \tag{14}$$

From the definition of output abstraction (Definition 3), it is easy to see that:

$$\begin{aligned} -\bar{\delta}_i &\leq \bar{y}_i - \bar{y}_{r_i} = E(i, :)(y - y_r) \leq \bar{\delta}_i, \\ \bar{\delta}_i &= \sum_{j=1}^p |\gamma_{ij}| \delta_j. \end{aligned} \quad (15)$$

Using (15) and the Cauchy-Schwarz inequality yields:

$$\begin{aligned} \sum_{i=1}^p \lambda_i (\bar{y}_i - \bar{y}_{r_i})^2 &\leq \Delta_R^2 = \sum_{i=1}^p \lambda_i \bar{\delta}_i^2, \\ \sum_{i=1}^p 2\lambda_i \bar{y}_{r_i} (\bar{y}_i - \bar{y}_{r_i}) &\leq 2\Delta_R \sqrt{\sum_{i=1}^p \lambda_i \bar{y}_{r_i}^2}, \\ \sum_{i=1}^p 2\lambda_i \bar{y}_i (\bar{y}_{r_i} - \bar{y}_i) &\leq 2\Delta_R \sqrt{\sum_{i=1}^p \lambda_i \bar{y}_i^2}. \end{aligned} \quad (16)$$

Combining the first and second inequality of (16) leads to:

$$\sum_{i=1}^p \lambda_i \bar{y}_i^2 \leq \left(\sqrt{\sum_{i=1}^p \lambda_i \bar{y}_{r_i}^2} + \Delta_R \right)^2. \quad (17)$$

Similarly, combining the first and the third inequality of (16) yields:

$$\sum_{i=1}^p \lambda_i \bar{y}_{r_i}^2 \leq \left(\sqrt{\sum_{i=1}^p \lambda_i \bar{y}_i^2} + \Delta_R \right)^2. \quad (18)$$

From (14), (17), and (18), we have:

$$\begin{aligned} \sqrt{(y - a)^T Q (y - a)} &\leq \sqrt{(y_r - a)^T Q (y_r - a)} + \Delta_R, \\ \sqrt{(y - a)^T Q (y - a)} &\geq \sqrt{(y_r - a)^T Q (y_r - a)} - \Delta_R. \end{aligned} \quad (19)$$

Using (19), we can conclude that $S(M_k^\delta)$ and $S(M_k^\delta)$ defined in Lemma 3 satisfy the safety relation (1), which completes the proof.